ARTICLE

doi:10.1038/nature13035

Haematopoietic stem cells require a highly regulated protein synthesis rate

Robert A. J. Signer[1], Jeffrey A. Magee[1], Adrian Salic[2] & Sean J. Morrison[1]

Many aspects of cellular physiology remain unstudied in somatic stem cells, for example, there are almost no data on protein synthesis in any somatic stem cell. Here we set out to compare protein synthesis in haematopoietic stem cells (HSCs) and restricted haematopoietic progenitors. We found that the amount of protein synthesized per hour in HSCs *in vivo* was lower than in most other haematopoietic cells, even if we controlled for differences in cell cycle status or forced HSCs to undergo self-renewing divisions. Reduced ribosome function in *Rpl24*$^{Bst/+}$ mice further reduced protein synthesis in HSCs and impaired HSC function. *Pten* deletion increased protein synthesis in HSCs but also reduced HSC function. *Rpl24*$^{Bst/+}$ cell-autonomously rescued the effects of *Pten* deletion in HSCs; blocking the increase in protein synthesis, restoring HSC function, and delaying leukaemogenesis. *Pten* deficiency thus depletes HSCs and promotes leukaemia partly by increasing protein synthesis. Either increased or decreased protein synthesis impairs HSC function.

Mutations in ribosomes and other gene products that affect protein synthesis are associated with human diseases marked by haematopoietic dysfunction[1,2]. Increased protein synthesis can promote the development and progression of certain cancers, including haematopoietic malignancies[3–6]. Ribosomal defects commonly impair HSC and erythroid progenitor function[7–11]. However, it is not clear whether these defects reflect a catastrophic reduction in protein synthesis below the level required for cellular homeostasis or whether HSCs require highly regulated protein synthesis.

Methods for measuring protein synthesis have depended upon the incorporation of radiolabelled amino acids, amino acid analogues[12], or puromycin[13–15] into nascent polypeptides in cultured cells. However, somatic stem cells profoundly change their properties in culture[16] necessitating the analysis of protein synthesis in rare cells *in vivo*. A new fluorogenic assay using O-propargyl-puromycin (OP-Puro) has been developed to image protein synthesis *in vivo*[17]. OP-Puro, like puromycin, is taken up by cells *in vivo*, entering ribosome acceptor sites and incorporating into nascent polypeptides[17]. An azide-alkyne reaction can be used to label OP-Puro fluorescently to quantitate protein synthesis in individual cells[17]. We adapted this approach to quantify protein synthesis by haematopoietic cells using flow cytometry.

HSCs synthesize less protein per hour

We administered a single intraperitoneal injection of OP-Puro (50 mg kg^{-1} body mass) then killed mice 1 h later and isolated bone marrow cells. We did not detect toxicity, signs of illness, changes in bone marrow cellularity, or changes in the frequencies of CD150^{+}CD48^{-}Lineage^{-}Sca-1^{+}c-kit^{+} (CD150^{+}CD48^{-}LSK) HSCs[18], annexin V^{+} bone marrow cells, annexin V^{+} HSCs, or dividing HSCs (Extended Data Fig. 1a–e).

Bone marrow cells from OP-Puro-treated mice showed a clear increase in fluorescence relative to untreated mice (Fig. 1a). The translation inhibitor cycloheximide profoundly blocked OP-Puro incorporation by bone marrow cells in culture (Fig. 1b). Incorporation of the methionine analogues, L-homopropargylglycine (HPG) and L-azidohomoalanine (AHA), into bone marrow cells, common myeloid progenitors (CMPs), granulocyte-macrophage progenitors (GMPs) and Gr-1^{+} myeloid cells correlated with OP-Puro incorporation in culture (Fig. 1c–f).

HSCs incorporated less OP-Puro than most other bone marrow cells from the same mice (Fig. 1g). This suggested that HSCs synthesize less protein per hour than most other haematopoietic progenitors. CD150^{-}CD48^{-}LSK multipotent progenitors (MPPs)[19] showed similar OP-Puro incorporation as HSCs (Fig. 1h); however, the mean rate of OP-Puro incorporation was significantly higher in unfractionated bone marrow cells, CMPs, GMPs, megakaryocyte-erythroid progenitors (MEPs), Gr-1^{+} myeloid cells, B220^{+}IgM^{-}CD43^{+} pro-B cells, B220^{+}IgM^{-}CD43^{-} pre-B cells, B220^{+}IgM^{+} B cells, CD3^{+} T cells, and CD71^{+}Ter119^{+} erythroid progenitors (Fig. 1h). Extended Data Figure 1f–i shows markers, gating strategies and OP-Puro incorporation histograms for each cell population.

To test whether reduced OP-Puro incorporation into HSCs reflects OP-Puro efflux by the Abcg2 transporter (also known as Bcrp1) we administered OP-Puro to *Abcg2*-deficient mice, which lack efflux activity in HSCs[20]. *Abcg2*$^{-/-}$ HSCs continued to show significantly lower mean rates of OP-Puro incorporation compared to most other *Abcg2*$^{-/-}$ progenitors (Fig. 2a), similar to the lowest levels observed among bone marrow cells (Fig. 2b).

Differences in OP-Puro incorporation did not reflect proteasomal degradation[21]. The maximum OP-Puro signal in haematopoietic cells was 1 h after OP-Puro administration (data not shown). However, HSCs showed little decline in OP-Puro signal between 1 and 3 h after administration and had significantly less OP-Puro incorporation than any restricted progenitor at both times (Fig. 2c). In contrast, the OP-Puro signal was profoundly reduced 24 h after administration (Fig. 2c). This suggested that degradation of OP-Puro-containing polypeptides requires several hours. Consistent with this, incubation of bone marrow cells at 37 °C for 30 min did not significantly reduce OP-Puro fluorescence in any cell population relative to an aliquot of the same cells kept on ice to arrest degradation (Extended Data Fig. 2a).

We pre-treated mice with bortezomib (1 mg kg^{-1}; intravenous) to inhibit proteasome activity[22] 1 h before OP-Puro administration. This significantly increased the OP-Puro signal in nearly all cell populations 24 h after OP-Puro administration (Extended Data Fig. 2b). When we assessed OP-Puro incorporation 1 h after administration, bortezomib pre-treatment only modestly increased OP-Puro fluorescence in certain

[1]Howard Hughes Medical Institute, Children's Research Institute, Department of Pediatrics, University of Texas Southwestern Medical Center, Dallas, Texas 75390, USA. [2]Department of Cell Biology, Harvard Medical School, Boston, Massachusetts 02115, USA.

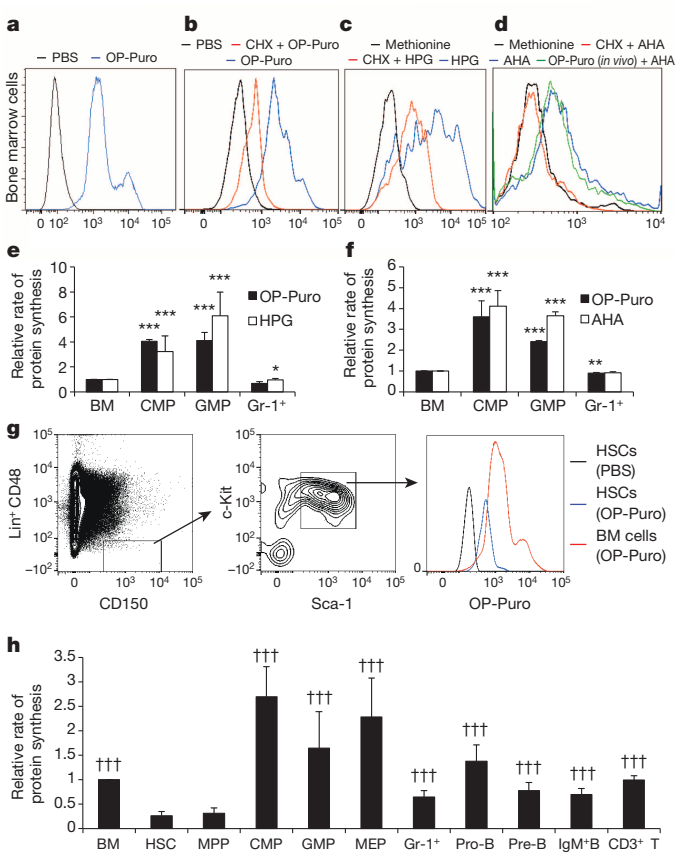

Figure 1 | Quantification of protein synthesis in haematopoietic cells *in vivo*. **a**, OP-Puro incorporation in bone marrow (BM) cells *in vivo* 1 h after administration. **b**–**d**, OP-Puro (**b**), HPG (**c**), and AHA (**d**) incorporation in bone marrow cells in culture was inhibited by cycloheximide (CHX). **d**, Bone marrow cells from mice treated with OP-Puro *in vivo* exhibited normal AHA incorporation in culture, indicating that OP-Puro did not block protein synthesis. **e**, **f**, OP-Puro versus HPG (**e**; $n = 4$ mice from 2 experiments) or AHA (**f**; $n = 3$ mice from 3 experiments) incorporation by haematopoietic cells in culture. **g**, OP-Puro incorporation in $CD150^{+}CD48^{-}$LSK HSCs and unfractionated bone marrow cells 1 h after administration *in vivo*. **h**, Protein synthesis in various haematopoietic stem cell and haematopoietic progenitor cell populations relative to unfractionated bone marrow cells ($n = 15$ mice from 9 experiments). Extended Data Fig. 1j shows the data from Fig. 1h using a $\log_2$ scale. Data represent mean ± s.d. Statistical significance was assessed using a two-tailed Student's *t*-tests (**e**, **f**) and differences relative to HSCs (**h**) were assessed using a repeated-measures one-way analysis of variance (ANOVA) followed by Dunnett's test for multiple comparisons. $*P < 0.05$, $**P < 0.01$, $***P < 0.001$ relative to bone marrow; $\dagger\dagger\dagger P < 0.001$ relative to HSCs in **h**.

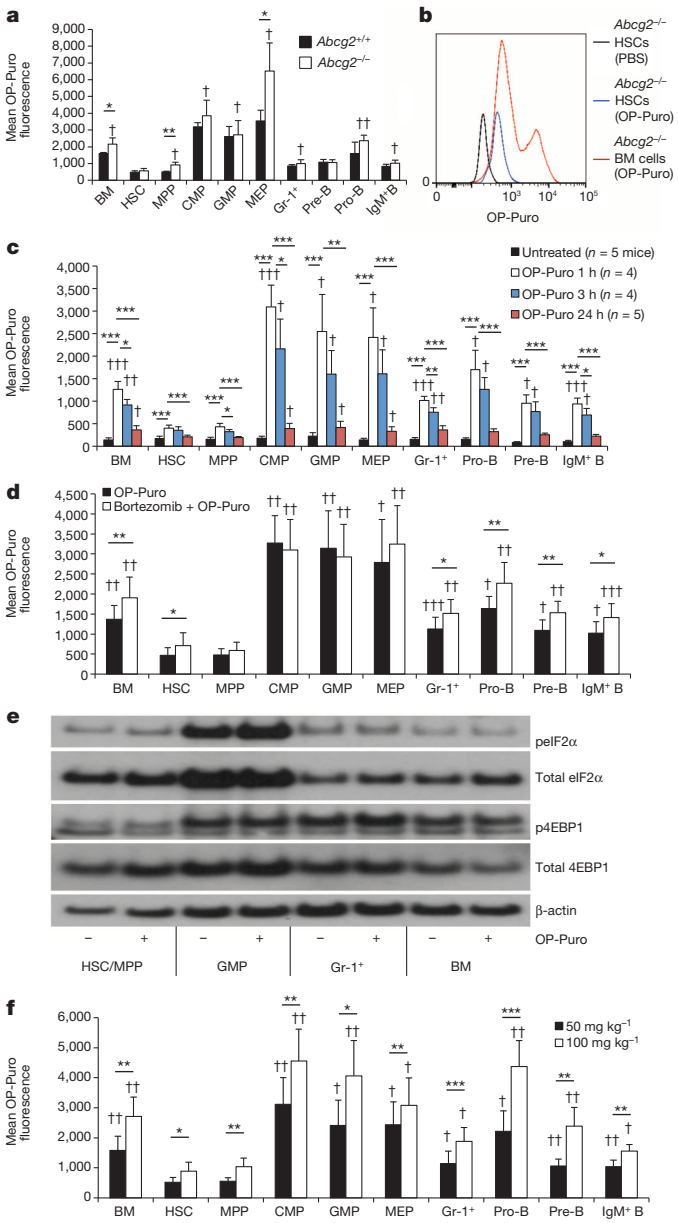

Figure 2 | Lower rate of OP-Puro incorporation by HSCs does not reflect efflux or proteasomal degradation. **a**, **b**, OP-Puro fluorescence in haematopoietic cells from *Abcg2*-deficient and control mice 1 h after OP-Puro administration *in vivo* ($n = 4$ mice from 3 experiments). **c**, OP-Puro fluorescence in haematopoietic cells 1, 3 or 24 h after OP-Puro administration ($n = 5$ experiments). **d**, OP-Puro fluorescence in haematopoietic cells 2 h after bortezomib and 1 h after OP-Puro administration *in vivo* ($n = 5$ mice per treatment from 5 experiments). **e**, Western blot analyses of 30,000 cells from each haematopoietic-cell population from OP-Puro-treated or control mice. **f**, OP-Puro fluorescence in haematopoietic cells 1 h after administering 50 mg kg^{-1} or 100 mg kg^{-1} OP-Puro ($n = 5$ mice per dose from 5 experiments). All data represent mean ± s.d. To assess the statistical significance of treatment effects within the same cells we performed two-tailed Student's *t*-tests; $*P < 0.05$, $**P < 0.01$, $***P < 0.001$. Differences between HSCs and other cell populations were assessed with a repeated-measures one-way ANOVA followed by Dunnett's test for multiple comparisons; $\dagger P < 0.05$, $\dagger\dagger P < 0.01$, $\dagger\dagger\dagger P < 0.001$.

cell populations (Fig. 2d). Even in the presence of bortezomib, HSCs had significantly less OP-Puro fluorescence than restricted progenitors. The lower OP-Puro incorporation by HSCs seems to primarily reflect reduced protein synthesis rather than accelerated proteasomal degradation.

OP-Puro also did not affect the levels of phosphorylated 4EBP1 or eIF2α (Fig. 2e), key regulators of translation that can be influenced by proteotoxic stress[23,24]. HSCs and MPPs had less phosphorylated 4EBP1 and β-actin per cell than other haematopoietic cells but similar levels of total 4EBP1. This raised the possibility that HSCs synthesize less protein as a consequence of increased 4EBP1-mediated inhibition of translation (Fig. 2e).

Doubling the dose of OP-Puro to 100 mg kg^{-1} significantly increased OP-Puro incorporation in all cell populations, but HSCs continued to have significantly lower levels than all other cell populations except MPPs (Fig. 2f). Thus, 50 mg kg^{-1} OP-Puro did not significantly attenuate protein synthesis and uptake was not saturated in HSCs or most other cells.

Dividing HSCs also make less protein

Haematopoietic progenitors in the replicating phases of the cell cycle (S, G_2 and M phases; S/G_2/M) exhibited significantly higher rates of OP-Puro incorporation than cells in G_0 and G_1 phases (G_0/G_1) (Fig. 3a, b). Total protein was also higher in Gr-1^{+} cells and bone marrow cells in

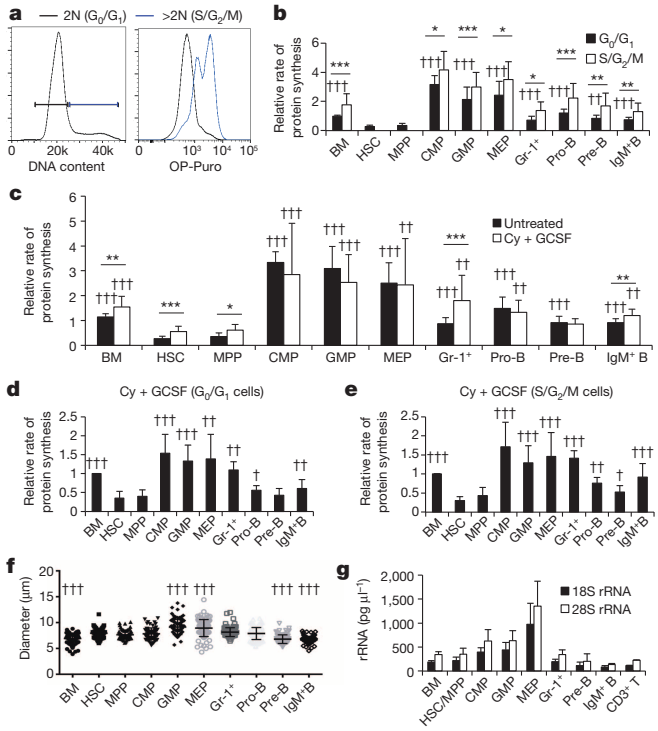

Figure 3 | HSCs synthesize less protein than most haematopoietic progenitors, even when undergoing self-renewing divisions. **a**, OP-Puro incorporation *in vivo* in bone marrow cells in G_0/G_1 versus $S/G_2/M$. 2N, diploid. **b**, Protein synthesis in G_0/G_1 and $S/G_2/M$ cells from haematopoietic-cell populations *in vivo* ($n = 10$ mice from 6 experiments). We were unable to assess OP-Puro incorporation in $S/G_2/M$ HSCs and MPPs in these experiments because these cells are very rare in normal bone marrow. **c**, Protein synthesis in haematopoietic cells after treatment with cyclophosphamide (Cy) and GCSF ($n = 10$ mice from 6 experiments). **d**, **e**, Protein synthesis in G_0/G_1 (**d**) and $S/G_2/M$ (**e**) cells from mice treated with Cy and GCSF ($n = 10$ mice from 6 experiments). Extended Data Fig. 3f, g shows the data from Fig. 3d, e side-by-side with data from untreated controls in Fig. 3b. **f**, Cell diameter ($n > 60$ cells per population from 2 mice). **g**, 18S rRNA and 28S rRNA content in 15,000 cells from each stem- or progenitor-cell population ($n = 3$ mice). All data represent mean ± s.d. To assess the statistical significance of treatment effects within the same cells (**b**, **c**), we performed two-tailed Student's *t*-tests; $*P < 0.05$, $**P < 0.01$, $***P < 0.001$. Differences between HSCs and other cells (**b**–**g**) were assessed with a repeated-measures one-way ANOVA followed by Dunnett's test for multiple comparisons; $\dagger P < 0.05$, $\dagger\dagger P < 0.01$, $\dagger\dagger\dagger P < 0.001$.

$S/G_2/M$ than in G_0/G_1 (Extended Data Fig. 3b). However, HSCs and MPPs exhibited less OP-Puro incorporation than restricted progenitors even when we compared only cells in G_0/G_1 (Fig. 3b). We treated mice with cyclophosphamide followed by two daily injections of granulocyte colony-stimulating factor (GCSF) to induce self-renewing divisions by HSCs (Extended Data Fig. 3d)[25]. Cyclophosphamide and GCSF also increased division by MPPs, Gr-1$^+$ cells and IgM$^+$ B cells (Extended Data Fig. 3a, e). Each of these populations showed increased OP-Puro incorporation after cyclophosphamide and GCSF treatment (Fig. 3c). However, HSCs had significantly less protein synthesis compared to most restricted progenitors, irrespective of whether we compared $S/G_2/M$ cells (Fig. 3e) or G_0/G_1 cells (Fig. 3d and Extended Data Fig. 3f, g) from mice treated with cyclophosphamide and GCSF.

Differences in protein synthesis between HSCs and restricted progenitors were not fully explained by differences in cell diameter (Fig. 3f and Extended Data Fig. 4b), ribosomal RNA (Fig. 3g and Extended Data Fig. 4c, d), or total RNA content (Extended Data Figs 3c and 4e), which were similar among HSCs and lymphoid progenitors despite differences in protein synthesis.

Ribosomal mutant impairs HSC function

Rpl24$^{Bst/+}$ mice have a hypomorphic mutation in the Rpl24 ribosome subunit, reducing protein synthesis in multiple cell types by 30% in culture[3,4,26]. Adult *Rpl24*$^{Bst/+}$ mice show relatively mild phenotypes: they are 20% smaller than wild-type mice and have mild pigmentation and skeletal abnormalities[26]. These *Rpl24*$^{Bst/+}$ mice had normal bone marrow, spleen and thymus cellularity, blood cell counts (Extended Data Fig. 5a, b) and HSC frequency (Fig. 4a). Frequencies of colony-forming progenitors (Extended Data Fig. 6b), restricted progenitors, and annexin V$^+$ HSCs and MPPs (Extended Data Fig. 5c–i) were also largely normal.

OP-Puro incorporation into unfractionated bone marrow cells, HSCs, GMPs and pre-B cells from *Rpl24*$^{Bst/+}$ mice was significantly reduced relative to wild-type cells (Fig. 4d). In the case of HSCs from *Rpl24*$^{Bst/+}$ mice, OP-Puro incorporation was reduced by approximately 30% relative to control HSCs. However, Rpl24 was highly differentially expressed

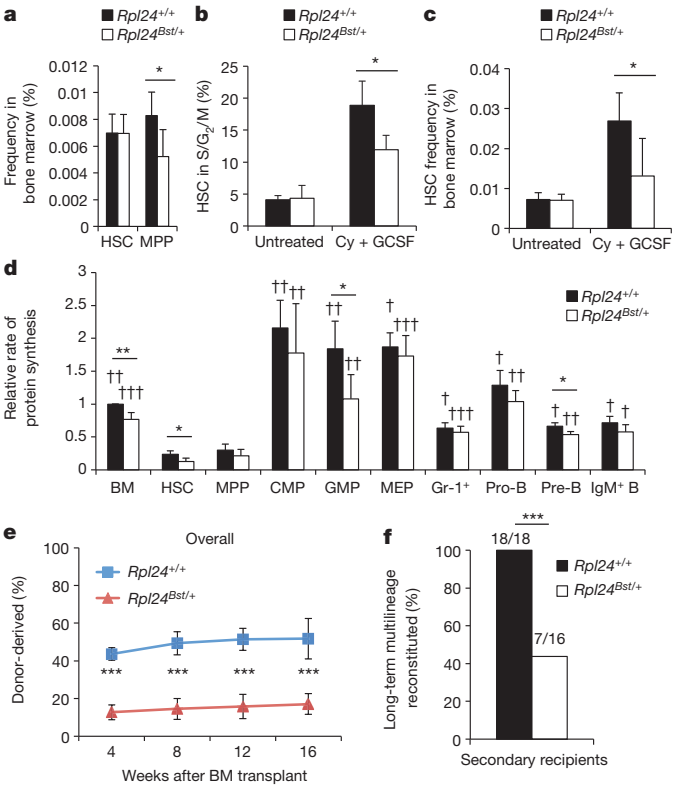

Figure 4 | *Rpl24*$^{Bst/+}$ HSCs synthesize less protein and have less capacity to reconstitute irradiated mice. **a**, Frequencies of HSCs and MPPs in *Rpl24*$^{Bst/+}$ ($n = 7$) versus littermate control ($n = 6$) mice ($n = 5$ experiments). **b**, **c**, Frequency of HSCs in $S/G_2/M$ (**b**; $n = 4$ untreated mice per genotype, $n = 4$ wild-type and 3 *Rpl24*$^{Bst/+}$ mice treated with Cy and GCSF in 3 experiments) and frequency of HSCs in the bone marrow (**c**; $n = 6$ wild-type and 7 *Rpl24*$^{Bst/+}$ untreated mice, $n = 7$ wild-type and 5 *Rpl24*$^{Bst/+}$ Cy-and GCSF-treated mice in 4 experiments) after treatment with Cy and GCSF. **d**, Protein synthesis in haematopoietic cells based on OP-Puro incorporation *in vivo* ($n = 4$ mice per genotype in 4 experiments). **e**, Donor-cell engraftment when 5×10^5 donor bone marrow cells were transplanted along with 5×10^5 recipient bone marrow cells into irradiated recipient mice ($n = 17$ recipient mice of wild-type bone marrow cells and 20 recipient mice of *Rpl24*$^{Bst/+}$ bone marrow cells in 4 experiments; myeloid-, B- and T-cell engraftment are shown in Extended Data Fig. 5k). **f**, The percentage of secondary recipients with long-term multilineage reconstitution (>0.5% donor myeloid and lymphoid cells for at least 16 weeks after transplantation) after secondary transplantation of 3×10^6 bone marrow cells from primary recipients in **e** ($n = 4$ donors per genotype). All data represent mean ± s.d. Statistical significance was assessed with two-tailed Student's *t*-tests (**a**–**e**) and Fisher's exact test (**f**); $*P < 0.05$, $**P < 0.01$, $***P < 0.001$. Differences between HSCs and other cell populations (**d**) were assessed with a repeated-measures one-way ANOVA followed by Dunnett's test for multiple comparisons; $\dagger P < 0.05$, $\dagger\dagger P < 0.01$, $\dagger\dagger\dagger P < 0.001$.

among haematopoietic cells and some cell populations seemed to depend more than others on Rpl24 for protein synthesis (Extended Data Fig. 5j).

After transplantation into irradiated mice, *Rpl24*$^{Bst/+}$ bone marrow cells gave significantly lower levels of donor cell reconstitution in the myeloid-, B- and T-cell lineages relative to control donor cells (Fig. 4e and Extended Data Fig. 5k). We did not detect impaired homing of *Rpl24*$^{Bst/+}$ LSK cells to the bone marrow (Extended Data Fig. 5l). Significantly impaired reconstitution by *Rpl24*$^{Bst/+}$ cells was also evident in secondary recipient mice (Fig. 4f). After cyclophosphamide and GCSF treatment, significantly fewer *Rpl24*$^{Bst/+}$ HSCs were in S/G_2/M than wild-type HSCs (Fig. 4b). HSC frequency in the bone marrow after cyclophosphamide and GCSF treatment was two- to threefold higher in wild-type than *Rpl24*$^{Bst/+}$ mice (Fig. 4c). Furthermore, colonies formed by individual *Rpl24*$^{Bst/+}$ HSCs in methylcellulose contained significantly fewer cells than wild-type HSC colonies (Extended Data Fig. 6c). *Rpl24*$^{Bst/+}$ HSCs are thus impaired in their proliferative potential.

Some ribosomal defects can induce p53 activation and expression of its target p21^{Cip1} (also known as Cdkn1a)[27]. When we compared *Rpl24*$^{Bst/+}$ with wild-type cells, we did not detect any difference in p53 levels among Lineage$^-$ haematopoietic progenitors (Extended Data Fig. 5m) or in p21^{Cip1} levels among LSK cells (Extended Data Fig. 5n). These data are consistent with previous studies[28] indicating that p53 and p21^{Cip1} are not induced in adult *Rpl24*$^{Bst/+}$ haematopoietic cells. Moreover, loss of a single allele of *p53* did not rescue the size of colonies formed by *Rpl24*$^{Bst/+}$ HSCs in culture (Extended Data Fig. 6e), even though p53 heterozygosity largely rescues developmental phenotypes in *Rpl24*$^{Bst/+}$ embryos[28]. HSC defects in *Rpl24*$^{Bst/+}$ mice are therefore not caused by increased p53 function.

Pten deletion increases protein synthesis

HSCs had phosphorylated Akt (pAkt) and pS6 levels that were similar to lymphoid progenitors but lower than myeloid progenitors (Fig. 5a and Extended Data Fig. 4f). We conditionally deleted *Pten* from adult haematopoietic cells in *Mx1-Cre; Pten*$^{fl/fl}$ mice. As shown previously[29–33], *Pten* deletion strongly increased pAKT and pS6 levels in bone marrow cells (Fig. 5a) and in HSCs and MPPs (Fig. 5d). Consistent with this, we observed an approximately 30% increase in protein synthesis in *Pten*-deficient relative to control HSCs ($P < 0.01$; Fig. 5b,c).

HSCs are depleted after *Pten* deletion, even after transplantation into wild-type recipients that never develop leukaemia, by a mechanism that depends on cell-autonomous mTORC1 and mTORC2 activation[29–32]. We examined OP-Puro incorporation into HSCs from *Mx1-Cre; Rictor*$^{fl/fl}$ mice, *Mx1-Cre; Rictor*$^{fl/fl}$; *Pten*$^{fl/fl}$ mice, and *Mx1-Cre; Pten*$^{fl/fl}$ mice. *Rictor* deletion (which inactivates mTORC2) had no effect on the rate of protein synthesis in otherwise wild-type HSCs (Fig. 5c and Extended Data Fig. 6g), consistent with the normal reconstituting capacity of *Rictor*-deficient HSCs[30]. However, *Rictor* deficiency significantly reduced protein synthesis in *Pten*-deficient HSCs to normal levels (Fig. 5c and Extended Data Fig. 6g). The ability of *Rictor* deletion to rescue both protein synthesis and HSC function after *Pten* deletion[30] suggested that *Pten* deletion depletes HSCs partly by cell-autonomously increasing protein synthesis. Rapamycin treatment, which also prevents HSC depletion after *Pten* deletion[31,32], also blocked the increase in protein synthesis in *Pten*-deficient HSCs (data not shown).

HSCs from *Mx1-Cre; Pten*$^{fl/fl}$; *Rpl24*$^{Bst/+}$ mice had significantly less protein synthesis than HSCs from *Mx1-Cre; Pten*$^{fl/fl}$ mice (Fig. 5b, c). Although ribosomes can promote mTORC2 signalling[34], *Rpl24*$^{Bst/+}$ did not reduce levels of pAKT, pGSK3β, pS6, or p4EBP1 in HSCs and MPPs (Fig. 5d), suggesting *Rpl24*$^{Bst/+}$ did not reduce mTORC1 or mTORC2 signalling. In fact, *Mx1-Cre; Pten*$^{fl/fl}$; *Rpl24*$^{Bst/+}$ HSCs and MPPs had slightly increased levels of pS6 and p4EBP1 relative to *Pten*-deficient HSCs and MPPs, but this would be expected to further increase protein synthesis rather than reducing it. This suggested that *Rpl24*$^{Bst/+}$ acted downstream of the PI3-kinase pathway to block the increase in protein synthesis in HSCs after *Pten* deletion, raising the question of whether *Rpl24*$^{Bst/+}$ could also block leukaemogenesis or HSC depletion.

Rpl24^{Bst} suppresses leukaemogenesis

Conditional deletion of *Pten* in haematopoietic cells leads to a myeloproliferative disorder (MPD) and T-cell acute lymphoblastic leukaemia (T-ALL)[31,33,35]. Increased protein synthesis promotes some haematopoietic malignancies, including T-cell leukaemias[3,4,6,36]. Two weeks after polyinosinic-polycytidylic acid (pIpC) administration, *Mx1-Cre; Pten*$^{fl/fl}$ mice showed significantly increased spleen and thymus cellularity (Fig. 5e, f and Extended Data Fig. 6h, i), consistent with the induction of MPD and T-ALL[31,33,35]. *Mx1-Cre; Pten*$^{fl/fl}$; *Rpl24*$^{Bst/+}$ mice exhibited normal spleen and thymus cellularity (Fig. 5e, f and Extended Data Fig. 6h, i), suggesting that reduced ribosome function impaired the development of MPD and T-ALL after *Pten* deletion.

To compare MPD and T-ALL development we transplanted 2×10^6 bone marrow cells from each genetic background into irradiated mice then treated with pIpC 4 weeks later. Recipients of *Mx1-Cre; Pten*$^{fl/fl}$; *Rpl24*$^{Bst/+}$ haematopoietic cells lived significantly longer than recipients of *Mx1-Cre; Pten*$^{fl/fl}$ haematopoietic cells (Fig. 5g). We confirmed by PCR that the donor cells had completely excised *Pten* (data not shown). When ill recipients of cells of either genotype were killed, they showed splenomegaly, thymomegaly and histological signs of MPD and T-ALL (Extended Data Fig. 6k). *Rpl24*$^{Bst/+}$ therefore significantly delayed ($P < 0.001$; Fig. 5g), but did not entirely prevent, MPD and T-ALL after *Pten* deletion. It is unclear whether *Rpl24*$^{Bst/+}$ impairs leukaemogenesis by acting within HSCs or within other haematopoietic cells.

Pten deletion mobilizes HSCs to the spleen[29,30]. *Rpl24*$^{Bst/+}$ blocked this effect, restoring normal HSC numbers in spleens of *Mx1-Cre; Pten*$^{fl/fl}$; *Rpl24*$^{Bst/+}$ mice (Extended Data Fig. 6j).

Rpl24^{Bst} rescues *Pten*–deficient HSCs

We performed long-term reconstitution assays in which we transplanted 10 CD150$^+$CD48$^-$LSK HSCs from wild-type, *Mx1-Cre; Pten*$^{fl/fl}$, *Rpl24*$^{Bst/+}$, or *Mx1-Cre; Pten*$^{fl/fl}$; *Rpl24*$^{Bst/+}$ mice along with 300,000 wild-type bone marrow cells into irradiated wild-type mice. As expected, most (15 of 18) recipients of wild-type HSCs but no (0 of 12) recipients of *Pten*-deficient HSCs showed long-term multilineage reconstitution by donor cells (Fig. 5h, i). Relative to control HSCs, *Rpl24*$^{Bst/+}$ HSCs gave lower levels of donor-cell reconstitution in all lineages (Fig. 5h) and a somewhat lower fraction of recipients showed long-term multilineage reconstitution (10 of 19; Fig. 5i), although these differences were not statistically significant. Relative to *Pten*-deficient HSCs, *Mx1-Cre; Pten*$^{fl/fl}$; *Rpl24*$^{Bst/+}$ compound mutant HSCs gave significantly higher levels of reconstitution and a significantly higher percentage of recipients showed long-term multilineage reconstitution by donor cells (Fig. 5h, i). Reconstitution by *Mx1-Cre; Pten*$^{fl/fl}$; *Rpl24*$^{Bst/+}$ HSCs was statistically indistinguishable from wild-type HSCs in all lineages except the B lineage (*Pten* deficiency impairs B-lineage progenitors independent of its effects on HSCs[33]; Fig. 5h). We confirmed by PCR that the donor cells had completely excised *Pten* (data not shown). This demonstrates that reducing protein synthesis restores the ability of *Pten*-deficient HSCs to give long-term multilineage reconstitution.

Secondary transplantation of 3×10^6 bone marrow cells from primary recipients with long-term multilineage reconstitution in Fig. 5h produced significantly less donor cell reconstitution and long-term multilineage reconstitution among recipients of *Rpl24*$^{Bst/+}$ compared to control HSCs (Fig. 5j, k). Secondary recipients of *Mx1-Cre; Pten*$^{fl/fl}$; *Rpl24*$^{Bst/+}$ compound mutant HSCs also showed significantly less donor cell reconstitution and long-term multilineage reconstitution compared to control HSCs. *Rpl24*$^{Bst/+}$ thus restored long-term multilineage reconstituting potential to *Pten*-deficient HSCs but did not fully restore wild-type function. *Pten* deficiency thus impairs HSC function, in part by increasing protein synthesis.

To test MPP function we competitively transplanted 100 donor CD150$^-$CD48$^-$LSK MPPs[19] from *Mx-1-Cre; Pten*$^{fl/fl}$, *Rpl24*$^{Bst/+}$, or control mice into irradiated recipients. There was a trend towards lower reconstitution by *Rpl24*$^{Bst/+}$ MPPs and *Pten*-deficient MPPs relative to control MPPs but the differences were not statistically significant

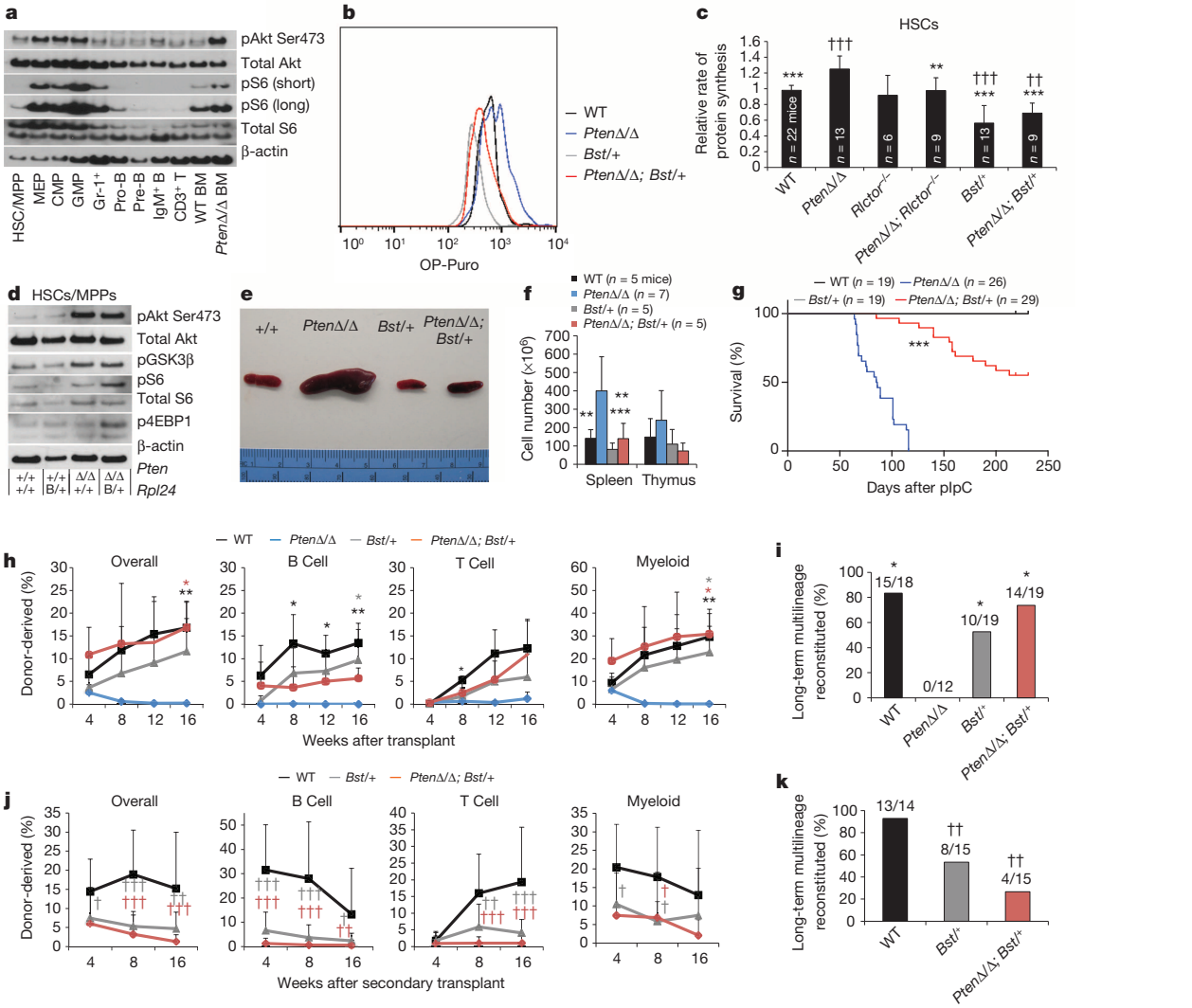

Figure 5 | *Rpl24*$^{Bst/+}$ blocks the increase in protein synthesis and restores HSC function after *Pten* deletion. **a**, Western blot analyses of 30,000 cells from each population. Long and short exposures for pS6 are shown. For total S6, a non-specific band is present below the specific band. Differences in β-actin represent differences in β-actin content per cell (one representative blot from two experiments). WT, wild type. **b**, Representative histograms of OP-Puro fluorescence in HSCs of each genotype. **c**, OP-Puro incorporation into HSCs of each genotype ($n = 15$ experiments). **d**, Western blot analyses of 30,000 CD48^{-}LSK cells (HSCs and MPPs) of the indicated genotypes (one representative blot from two experiments). **e**, Representative spleens 2 weeks after pIpC administration to wild-type, *Mx-1-Cre; Pten*$^{fl/fl}$ (*Pten*Δ/Δ), *Rpl24*$^{Bst/+}$ (*Bst*/+), and *Mx-1-Cre; Pten*$^{fl/fl}$; *Rpl24*$^{Bst/+}$ (*Pten*Δ/Δ; *Bst*/+) mice. **f**, Spleen and thymus cellularity ($n = 7$ experiments). **g**, Time until mice had to be euthanized owing to illness after transplantation of 2×10^6 bone marrow cells of the indicated genotypes into irradiated recipient mice. **h**, **i**, Ten donor HSCs were transplanted along with 3×10^5 recipient bone marrow cells into irradiated recipients. Donor-cell engraftment (**h**) and fraction of recipients that showed long-term multilineage reconstitution (**i**; 3 experiments). **j**, **k**, Donor-cell engraftment (**j**) and the fraction of secondary recipients that showed long-term multilineage reconstitution (**k**) after transplantation of 3×10^6 bone marrow cells from primary recipients in **h** ($n = 4$ donors per genotype). All data represent mean ± s.d. Differences among genotypes (**c**, **f**, **h**) were assessed with a one-way ANOVA followed by Dunnett's test for multiple comparisons. Statistical significance was assessed by log-rank test (**g**), chi-squared tests followed by Tukey's *t*-tests for pairwise comparisons (**i**, **k**), or a one-way ANOVA followed by Tukey's *t*-tests for multiple comparisons (**j**). Significance was expressed relative to wild-type (†$P < 0.05$, ††$P < 0.01$, †††$P < 0.001$) or *Pten*-deficient cells (*$P < 0.05$, **$P < 0.01$, ***$P < 0.001$).

(Extended Data Fig. 7a, b). Neither *Rpl24*$^{Bst/+}$ nor *Pten* deletion significantly affected the percentage of bone marrow cells that formed colonies or the cellularity of those colonies (Extended Data Fig. 6b, d). Thus, we have not detected clear effects of *Rpl24*$^{Bst/+}$ or *Pten* deletion on the proliferative potential of MPPs or restricted progenitors, suggesting that they are not as sensitive as HSCs to changes in protein synthesis, although it remains possible that they are also impaired by changes in protein synthesis.

DISCUSSION

When we added HSCs to culture, OP-Puro incorporation increased dramatically (data not shown). This raises the possibility that the failure to maintain HSCs sustainably under any known culture conditions[37] may reflect a limitation imposed by increased protein synthesis. Consistent with this, rapamycin promotes HSC maintenance in culture[38], although it remains to be determined whether rapamycin attenuates the increase in protein synthesis in cultured HSCs.

Low rates of protein synthesis may be essential for maintaining metabolic homeostasis in HSCs and potentially in other kinds of somatic stem cells. Changes in protein synthesis may cause undesirable changes in the quality and/or content of the proteome, such as due to misfolding. There may also be changes in the translation of certain subsets of transcripts (potentially including key HSC regulators) when protein synthesis increases, similar to what occurs in cancer cells[5].

Embryonic stem cells have high proteasome activity and proteasome activity increases both embryonic-stem-cell maintenance and *Caenorhabditis elegans* lifespan[39,40]. Rapamycin treatment, and mutations that reduce mTOR signalling, also increase lifespan (see citations in ref. 41) and would be predicted to reduce protein synthesis. In the context of these results, our observations raise the possibility that reduced protein synthesis and/or increased proteasome activity is required to maintain certain long-lived somatic cells in addition to increasing organismal lifespan.

METHODS SUMMARY

For *in vivo* quantification of protein synthesis, OP-Puro (50 mg kg^{-1}; pH 6.4–6.6 in PBS; Medchem Source) was injected intraperitoneally. Unless otherwise indicated, bone marrow was collected 1 h later and 3×10^6 cells were stained with antibodies against cell surface markers, fixed in 1% paraformaldehyde, and permeabilized in PBS with 3% fetal bovine serum and 0.1% saponin, as described in the Methods. OP-Puro was detected by performing an azide-alkyne cycloaddition with the Click-iT Cell Reaction Buffer Kit (Life Technologies), and analysed by flow cytometry as described in the Methods. 'Relative rates of protein synthesis' were calculated by normalizing OP-Puro signals to bone marrow after subtracting background fluorescence. 'Mean OP-Puro fluorescence' reflected absolute fluorescence values for each cell population from multiple experiments.

Online Content Any additional Methods, Extended Data display items and Source Data are available in the online version of the paper; references unique to these sections appear only in the online paper.

Received 4 May 2013; accepted 15 January 2014.
Published online 9 March 2014.

1. Narla, A. & Ebert, B. L. Ribosomopathies: human disorders of ribosome dysfunction. *Blood* **115,** 3196–3205 (2010).
2. Sakamoto, K. M., Shimamura, A. & Davies, S. M. Congenital disorders of ribosome biogenesis and bone marrow failure. *Biol. Blood Marrow Transplant.* **16,** S12–S17 (2010).
3. Hsieh, A. C. *et al.* Genetic dissection of the oncogenic mTOR pathway reveals druggable addiction to translational control via 4EBP-eIF4E. *Cancer Cell* **17,** 249–261 (2010).
4. Barna, M. *et al.* Suppression of Myc oncogenic activity by ribosomal protein haploinsufficiency. *Nature* **456,** 971–975 (2008).
5. Hsieh, A. C. *et al.* The translational landscape of mTOR signalling steers cancer initiation and metastasis. *Nature* **485,** 55–61 (2012).
6. Ruggero, D. & Pandolfi, P. P. Does the ribosome translate cancer? *Nature Rev. Cancer* **3,** 179–192 (2003).
7. Jaako, P. *et al.* Mice with ribosomal protein S19 deficiency develop bone marrow failure and symptoms like patients with Diamond–Blackfan anemia. *Blood* **118,** 6087–6096 (2011).
8. Wong, C. C., Traynor, D., Basse, N., Kay, R. R. & Warren, A. J. Defective ribosome assembly in Shwachman–Diamond syndrome. *Blood* **118,** 4305–4312 (2011).
9. Danilova, N., Sakamoto, K. M. & Lin, S. Ribosomal protein S19 deficiency in zebrafish leads to developmental abnormalities and defective erythropoiesis through activation of p53 protein family. *Blood* **112,** 5228–5237 (2008).
10. Sen, S. *et al.* The ribosome-related protein, SBDS, is critical for normal erythropoiesis. *Blood* **118,** 6407–6417 (2011).
11. Payne, E. M. *et al.* L–Leucine improves the anemia and developmental defects associated with Diamond-Blackfan anemia and del(5q) MDS by activating the mTOR pathway. *Blood* **120,** 2214–2224 (2012).
12. Beatty, K. E. *et al.* Fluorescence visualization of newly synthesized proteins in mammalian cells. *Angew. Chem. Int. Edn Engl.* **45,** 7364–7367 (2006).
13. Nathans, D. Puromycin inhibition of protein synthesis: incorporation of puromycin into peptide chains. *Proc. Natl Acad. Sci. USA* **51,** 585–592 (1964).
14. Schmidt, E. K., Clavarino, G., Ceppi, M. & Pierre, P. SUnSET, a nonradioactive method to monitor protein synthesis. *Nature Methods* **6,** 275–277 (2009).
15. Starck, S. R., Green, H. M., Alberola-Ila, J. & Roberts, R. W. A general approach to detect protein expression *in vivo* using fluorescent puromycin conjugates. *Chem. Biol.* **11,** 999–1008 (2004).
16. Joseph, N. M. & Morrison, S. J. Toward and understanding of the physiological function of mammalian stem cells. *Dev. Cell* 173–183 (2005).
17. Liu, J., Xu, Y., Stoleru, D. & Salic, A. Imaging protein synthesis in cells and tissues with an alkyne analog of puromycin. *Proc. Natl Acad. Sci. USA* **109,** 413–418 (2012).
18. Kiel, M. J. *et al.* SLAM family receptors distinguish hematopoietic stem and progenitor cells and reveal endothelial niches for stem cells. *Cell* **121,** 1109–1121 (2005).
19. Oguro, H., Ding, L. & Morrison, S. J. SLAM family markers resolve functionally distinct subpopulations of hematopoietic stem cells and multipotent progenitors. *Cell Stem Cell* **13,** 102–116 (2013).
20. Zhou, S. *et al. Bcrp1* gene expression is required for normal numbers of side population stem cells in mice, and confers relative protection to mitoxantrone in hematopoietic cells *in vivo*. *Proc. Natl Acad. Sci. USA* **99,** 12339–12344 (2002).
21. Ciechanover, A., Finley, D. & Varshavsky, A. Ubiquitin dependence of selective protein degradation demonstrated in the mammalian cell cycle mutant ts85. *Cell* **37,** 57–66 (1984).
22. Luker, G. D., Pica, C. M., Song, J., Luker, K. E. & Piwnica-Worms, D. Imaging 26S proteasome activity and inhibition in living mice. *Nature Med.* **9,** 969–973 (2003).
23. Gingras, A. C., Raught, B. & Sonenberg, N. Regulation of translation initiation by FRAP/mTOR. *Genes Dev.* **15,** 807–826 (2001).
24. Wek, R. C., Jiang, H. Y. & Anthony, T. G. Coping with stress: eIF2 kinases and translational control. *Biochem. Soc. Trans.* **34,** 7–11 (2006).
25. Morrison, S. J., Wright, D. & Weissman, I. L. Cyclophosphamide/granulocyte colony-stimulating factor induces hematopoietic stem cells to proliferate prior to mobilization. *Proc. Natl Acad. Sci. USA* **94,** 1908–1913 (1997).
26. Oliver, E. R., Saunders, T. L., Tarle, S. A. & Glaser, T. Ribosomal protein L24 defect in belly spot and tail (*Bst*), a mouse *Minute*. *Development* **131,** 3907–3920 (2004).
27. Fumagalli, S. & Thomas, G. The role of p53 in ribosomopathies. *Semin. Hematol.* **48,** 97–105 (2011).
28. Barkić, M. *et al.* The p53 tumor suppressor causes congenital malformations in *Rpl24*-deficient mice and promotes their survival. *Mol. Cell. Biol.* **29,** 2489–2504 (2009).
29. Lee, J. Y. *et al.* mTOR activation induces tumor suppressors that inhibit leukemogenesis and deplete hematopoietic stem cells after *Pten* deletion. *Cell Stem Cell* **7,** 593–605 (2010).
30. Magee, J. A. *et al.* Temporal changes in PTEN and mTORC2 regulation of hematopoietic stem cell self-renewal and leukemia suppression. *Cell Stem Cell* **11,** 415–428 (2012).
31. Yilmaz, O. H. *et al.* Pten dependence distinguishes haematopoietic stem cells from leukaemia-initiating cells. *Nature* **441,** 475–482 (2006).
32. Kalaitzidis, D. *et al.* mTOR Complex 1 plays critical roles in hematopoiesis and pten-loss-evoked leukemogenesis. *Cell Stem Cell* **11,** 429–439 (2012).
33. Zhang, J. *et al.* PTEN maintains haematopoietic stem cells and acts in lineage choice and leukaemia prevention. *Nature* **441,** 518–522 (2006).
34. Zinzalla, V., Stracka, D., Oppliger, W. & Hall, M. N. Activation of mTORC2 by association with the ribosome. *Cell* **144,** 757–768 (2011).
35. Guo, W. *et al.* Multi-genetic events collaboratively contribute to *Pten*-null leukaemia stem-cell formation. *Nature* **453,** 529–533 (2008).
36. Ruggero, D. Translational control in cancer etiology. *Cold Spring Harb. Perspect. Biol.* **5,** a012336 (2013).
37. Dahlberg, A., Delaney, C. & Bernstein, I. D. *Ex vivo* expansion of human hematopoietic stem and progenitor cells. *Blood* **117,** 6083–6090 (2011).
38. Huang, J., Nguyen-McCarty, M., Hexner, E. O., Danet-Desnoyers, G. & Klein, P. S. Maintenance of hematopoietic stem cells through regulation of Wnt and mTOR pathways. *Nature Med.* **18,** 1778–1785 (2012).
39. Vilchez, D. *et al.* Increased proteasome activity in human embryonic stem cells is regulated by PSMD11. *Nature* **489,** 304–308 (2012).
40. Vilchez, D. *et al.* RPN-6 determines *C. elegans* longevity under proteotoxic stress conditions. *Nature* **489,** 263–268 (2012).
41. Signer, R. A. & Morrison, S. J. Mechanisms that regulate stem cell aging and life span. *Cell Stem Cell* **12,** 152–165 (2013).

Acknowledgements S.J.M. is a Howard Hughes Medical Institute Investigator, the Mary McDermott Cook Chair in Pediatric Genetics, and the director of the Hamon Laboratory for Stem Cells and Cancer. This work was supported by the Cancer Prevention and Research Institute of Texas and the National Institute on Aging (R37 AG024945). R.A.J.S. was supported by fellowships from the Leukemia & Lymphoma Society (5541-11) and the Canadian Institutes of Health Research (MFE-106993). J.A.M. was supported by the UT Southwestern K12 Pediatrics Training Grant (K12-HD068369). We thank A. Pineda, K. Cowan, E. Daniel, M. Acar, H. Oguro, J. Peyer, K. Rajagopalan, M. Agathocleous and E. Piskounova for technical support and advice; N. Loof and the Moody Foundation Flow Cytometry Facility, L. Hynan and J. Reisch for advice regarding statistics; J. Shelton for histology; and R. Coolon, S. Manning, M. Gross and K. Correll for mouse colony management.

Author Contributions R.A.J.S. conceived the project. A.S. developed the OP-Puro reagent and provided advice in the early stages of the project. R.A.J.S. performed all of the experiments with the exception of the western blot analyses in Figs 2e and 5a, d, and Extended Data Fig. 5j, which were performed by J.A.M. R.A.J.S., J.A.M. and S.J.M. designed the experiments and interpreted results. R.A.J.S. and S.J.M. wrote the manuscript.

Author Information Reprints and permissions information is available at www.nature.com/reprints. The authors declare no competing financial interests. Readers are welcome to comment on the online version of the paper. Correspondence and requests for materials should be addressed to S.J.M. (sean.morrison@utsouthwestern.edu).

METHODS

Mice. *Rpl24*$^{Bst/+}$ (ref. 26), *Pten*$^{fl/fl}$ (ref. 42), *Mx1-Cre* (ref. 43), *Rictor*$^{fl/fl}$ (ref. 30), *Abcg2*$^{-/-}$ (ref. 44) and *p53*$^{+/-}$ (ref. 45) mutant mice have been described previously. These mice were all backcrossed for at least eight generations onto a C57BL background, with the exception of *Abcg2*$^{-/-}$ mice, which were on an FVB.129 N7 background (Taconic). C57BL/Ka-Thy-1.1 (CD45.2) and C57BL/Ka-Thy-1.2 (CD45.1) mice were used in transplantation experiments. Both male and female mice were used in all studies. Expression of *Mx1-Cre* was induced by three or four intraperitoneal injections of 10 μg pIpC (GE Healthcare) administered every other day, beginning at approximately 6 weeks of age. For cyclophosphamide and GCSF experiments, 4 mg of cyclophosphamide (Baxter) was administered by intraperitoneal injection on day 0, and 5 μg of GCSF (Neupogen; Amgen) was administered by subcutaneous injection on days 1 and 2. Mice were analysed on day 3. All mice were housed in the Unit for Laboratory Animal Medicine at the University of Michigan, where breeding for these studies was initiated, or in the Animal Resource Center at the University of Texas Southwestern Medical Center, where these studies were performed. All protocols were approved by the University of Michigan Committee on the Use and Care of Animals and by the University of Texas Southwestern Institutional Animal Care and Use Committee.

Measurement of protein synthesis. For *in vitro* analysis 10^3–10^4 bone marrow or sorted cells were plated in 100 μl of methionine-free Dulbecco's Modified Eagle's Medium (Sigma) supplemented with 200 μM L-cysteine (Sigma), 50 μM 2-mercaptoethanol (Sigma), 1 mM L-glutamine (Gibco) and 0.1% bovine serum albumin (BSA; Sigma). For analysis of HPG and AHA incorporation, cells were pre-cultured for 45 min to deplete endogenous methionine. For OP-Puro, the medium was supplemented with 1 mM L-methionine (Sigma). HPG (Life Technologies; 1 mM final concentration), AHA (Life Technologies; 1 mM final concentration) or OP-Puro (Medchem Source; 50 μM final concentration) were added to the culture medium for 1 h (HPG and OP-Puro) or 2.5 h (AHA), then cells were removed from wells and washed twice in Ca^{2+}- and Mg^{2+}-free phosphate buffered saline (PBS). Cells were fixed in 0.5 ml of 1% paraformaldehyde (Affymetrix) in PBS for 15 min on ice. Cells were washed in PBS, then permeabilized in 200 μl PBS supplemented with 3% fetal bovine serum (Sigma) and 0.1% saponin (Sigma) for 5 min at room temperature (20–25 °C). The azide-alkyne cycloaddition was performed using the Click-iT Cell Reaction Buffer Kit (Life Technologies) and azide conjugated to Alexa Fluor 488 or Alexa Fluor 555 (Life Technologies) at 5 μM final concentration. After the 30-min reaction, the cells were washed twice in PBS supplemented with 3% fetal bovine serum and 0.1% saponin, then resuspended in PBS supplemented with 4′,6-diamidino-2-phenylindole (DAPI; 4 μg ml^{-1} final concentration) and analysed by flow cytometry. To inhibit OP-Puro, HPG or AHA incorporation, cycloheximide (Sigma) was added 30 min before OP-Puro, HPG or AHA at a final concentration of 100 μg ml^{-1}. All cultures were incubated at 37 °C in 6.5% CO_2 and constant humidity.

For *in vivo* analysis, OP-Puro (50 mg kg^{-1} body mass; pH 6.4–6.6 in PBS) was injected intraperitoneally. One hour later mice were euthanized, unless indicated otherwise. Bone marrow was collected, and 3×10^6 cells were stained with combinations of antibodies against cell-surface markers as described below. After washing, the cells were fixed, permeabilized, and the azide-alkyne cycloaddition was performed as described above. 'Relative rates of protein synthesis' were calculated by normalizing OP-Puro signals to whole bone marrow after subtracting autofluorescence background. 'Mean OP-Puro fluorescence' reflected absolute fluorescence values for each cell population from multiple independent experiments.

To assess the effect of proteasome activity on OP-Puro incorporation mice were administered an intravenous injection of bortezomib (Cell Signaling; 1 mg kg^{-1} body mass) 1 h before OP-Puro administration. OP-Puro incorporation was assessed as described above 1 h later unless indicated otherwise.

Flow cytometry and cell isolation. Bone marrow cells were isolated by flushing the long bones (femurs and tibias) or by crushing the long bones, vertebrae and pelvic bones with a mortar and pestle in Ca^{2+}- and Mg^{2+}-free Hank's buffered salt solution (HBSS; Gibco) supplemented with 2% heat-inactivated bovine serum (Gibco). Spleens and thymuses were prepared by crushing tissues between frosted slides. All cells were filtered through a 40-μm cell strainer to obtain single cell suspensions. Cell number and viability were assessed by a Vi-CELL cell viability analyser (Beckman Coulter) or by counting with a hemocytometer.

For flow cytometric analysis and isolation of specific haematopoietic progenitors, cells were incubated with combinations of antibodies to the following cell-surface markers, conjugated to FITC, PE, PerCP-Cy5.5, Cy5, APC, PE-Cy7, eFluor 660, Alexa Fluor 700, APC-eFluor 780 or biotin (antibodies are given in brackets in the following list): CD2 (RM2-5), CD3ε (17A2), CD4 (GK1.5), CD5 (53-7.3), CD8α (53-6.7), CD11b (M1/70), CD16/32 (FcYRII/III; 93), CD24 (M1/69), CD25 (PC61.5), CD34 (RAM34), CD43 (1B11), CD44 (IM7), CD45.1 (A20), CD45.2 (104), CD45R (B220; RA3-6B2), CD48 (HM48-1), CD71 (C2), CD117 (cKit; 2B8), CD127 (IL7Rα; A7R34), CD138 (281-2), CD150 (TC15-12F12.2), Ter119 (TER-119), Sca-1 (D7, E13-161.7), Gr-1 (RB6-8C5) and IgM (II/41). For isolation of HSCs and MPPs, Lineage markers included CD3, CD5, CD8, B220, Gr-1 and Ter119. For isolation of CMPs, GMPs and MEPs, these Lineage markers were supplemented with additional antibodies against CD4 and CD11b.

Biotinylated antibodies were visualized by incubation with PE-Cy7 or APC-Alexa Fluor 750 conjugated streptavidin. All reagents were acquired from BD Biosciences, eBiosciences, or BioLegend. All incubations were for approximately 30 min on ice. HSCs, MPPs, CD34$^+$CD16/32^{low}CD127$^-$Lineage$^-$Sca-1$^-$c-kit$^+$ CMPs (ref. 46), CD34$^+$CD16/32^{high}CD127$^-$Lineage$^-$Sca-1$^-$c-kit$^+$ GMPs (ref. 46), and CD34$^-$CD16/32$^{-/low}$CD127$^-$Lineage$^-$Sca-1$^-$c-kit$^+$ MEPs (ref. 46) were sometimes pre-enriched by selecting c-kit$^+$ cells using paramagnetic microbeads and an autoMACS magnetic separator (Miltenyi Biotec).

Non-viable cells were excluded from sorts and analyses using DAPI (4′,6-diamidino-2-phenylindole). Apoptotic cells were identified using APC annexin V (BD Biosciences). Data acquisition and cell sorting were performed on a FACSAria flow cytometer (BD Biosciences). All sorted fractions were double sorted to ensure high purity. Data were analysed by FACSDiva (BD Biosciences) or FlowJo (Tree Star) software.

Long-term competitive repopulation assay. Adult recipient mice (CD45.1) were administered a minimum lethal dose of radiation using an XRAD 320 X-ray irradiator (Precision X-Ray) to deliver two doses of 540 rad (1,080 rad in total) at least 3 h apart. Cells were injected into the retro-orbital venous sinus of anaesthetized recipients. For competitive bone marrow transplants 5×10^5 donor and 5×10^5 recipient cells were transplanted. For HSC transplants 10 donor CD150$^+$CD48$^-$Lineage$^-$Sca-1$^+$c-kit$^+$ HSCs and 3×10^5 recipient bone marrow cells were transplanted. Blood was obtained from the tail veins of recipient mice every 4 weeks for at least 16 weeks after transplantation. For MPP transplants 100 donor CD150$^-$CD48$^-$Lineage$^-$Sca-1$^+$c-kit$^+$ MPPs and 3×10^5 recipient bone marrow cells were transplanted. Blood was obtained from the tail veins of recipient mice 3, 5 and 7 weeks after transplantation. Red blood cells were lysed with ammonium chloride potassium buffer. The remaining cells were stained with antibodies against CD45.2, CD45.1, CD45R (B220), CD11b, CD3 and Gr-1 to assess donor-cell engraftment. Mice that died or developed obvious haematopoietic neoplasms were omitted from the analyses. For secondary transplants, 3×10^6 bone marrow cells collected from primary recipients were transplanted non-competitively into irradiated recipient mice. Primary recipients used for secondary transplantation had long-term multilineage reconstitution by donor cells and levels of donor-cell reconstitution that were typical (closest to mean values) for the treatments from which they originated. For survival studies in Fig. 5, irradiated mice were transplanted with 2×10^6 bone marrow cells of each genotype and pIpC was administered 4 weeks later to delete *Pten*. Three to four donors per genotype were used with 5 to 10 recipients per donor. Mice were euthanized when they appeared moribund.

Western blot analysis. Equal numbers of cells from each stem or progenitor population (unless indicated otherwise) were sorted into, or resuspended in, trichloracetic acid (TCA, Sigma). The final concentration was adjusted to 10% TCA. Extracts were incubated on ice for at least 15 min and centrifuged at 16,100*g* at 4 °C for 15 min. Precipitates were washed in acetone twice and dried. The pellets were solubilized in 9 M urea, 2% Triton X-100, and 1% DTT. LDS loading buffer (Life Technologies) was added and the pellet was heated at 70 °C for 10 min. Samples were separated on Bis-Trispolyacrylamide gels (Life Technologies) and transferred to PVDF membranes (Millipore). Western blot analyses were performed according to the protocol from Cell Signaling Technologies and blots were developed with the SuperSignal West Femto chemiluminescence kit (Thermo Scientific). Blots were stripped with 1% SDS, 25 mM glycine (pH 2) before re-probing. The following primary antibodies were used for western blot analyses (obtained from Cell Signaling Technologies unless indicated otherwise): phos-Akt (Ser473; D9E), AKT (C67E7), phos-S6 (Ser240/244; polyclonal), S6 (5G10), phos-4E-BP1 (Thr37/46; 236B4), 4E-BP1 (polyclonal), phos-eIF2α (Ser51; polyclonal), eIF2α (D7D3), phos-GSK3β (Ser9; D85E12), β-actin (AC-74; Sigma), p53 (cm5p; Leica), p21^{Cip1} (F-5; Santa Cruz) and Rpl24 (polyclonal; Abcam). For p21^{Cip1}, the membranes were treated with the SuperSignal Western Blot Enhancer (Thermo Scientific). Band intensity was quantified with ImageJ software.

Methylcellulose cultures. Two-hundred live bone marrow cells or single CD150$^+$CD48$^-$LSK cells were sorted per well of a 96-well plate containing methylcellulose culture medium (M3434, StemCell Technologies) and incubated at 37 °C in 6.5% CO_2 and constant humidity. Colony formation was assessed 14 days after plating, except for data shown in Extended Data Fig. 6e, in which colonies were assessed 15 days after plating. Colony size was assessed by picking individual colonies with a pipette under the microscope, washing the cells in PBS, and counting live cells by Trypan blue exclusion on a hemocytometer.

Cell size. The average diameter of sorted cells was measured by sorting cells into flat-bottom 96-well plates and analysing micrographs with ImageJ software.

RNA content. From each haematopoietic-cell population, 15,000 cells were sorted into RLT Plus buffer (Qiagen) supplemented with 2-mercaptoethanol. RNA from each sample was extracted with the RNeasy micro plus kit (Qiagen) into 14 μl of water. Two microlitres of each sample were analysed in duplicate for 18S rRNA, 28S rRNA and total RNA concentration using an Agilent RNA 6000 Pico kit and a Bioanalyzer (Agilent) at the University of Texas Southwestern Genomics and Microarray Core.

Protein content. From each population, 50,000 cells were sorted into PBS. G_0/G_1 cells were distinguished from $S/G_2/M$ cells based on DNA content using Hoechst 33342 (Sigma) staining of live cells. Cells were spun down and resuspended in 20 μl of RIPA buffer (Pierce) supplemented with complete protease inhibitor (Roche) and rotated at 4 °C for 30 min. Lysates were spun down at 16,100*g* at 4 °C for 15 min. The protein content in the supernatant was assessed with the BCA assay (Pierce).

Statistical methods. In all cases, multiple independent experiments were performed on different days to verify the reproducibility of experimental findings. Group data are always represented by mean ± standard deviation. The numbers of experiments noted in figure legends reflect independent experiments performed on different days.

To test statistical significance between two samples, two-tailed Student's *t*-tests were used. When multiple samples were compared, statistical significance was assessed using a one-way ANOVA or a repeated-measures one-way ANOVA (when comparing multiple time points or populations from the same mouse) followed by Dunnett's test for multiple comparisons. When multiple samples were each compared to one another, statistical significance was assessed using a one-way ANOVA followed by Tukey's *t*-tests for multiple comparisons. Statistical significance comparing overall numbers of mice with long-term multilineage reconsitution was assessed either by a Fisher's exact test (Fig. 4f) or by chi-squared tests followed by Tukey's *t*-tests for pairwise comparisons (Fig. 5i, k). Statistical significance with respect to differences in survival (Fig. 5g) was calculated using a log-rank test. The specific type of test used for each figure panel is described in the figure legends.

For normalized protein synthesis rates and normalized messenger RNA expression, means were calculated and statistical tests were performed using $\log_{10}$-transformed data and then means were back-transformed to prevent data skewing.

No randomization or blinding was used in any experiments. The only mice excluded from any experiment were those that developed leukaemia after transplantation in Fig. 5h, i. As the purpose of this experiment was to compare the reconstituting capacity of normal HSCs, the presence of leukaemia in a minority of recipient mice was a confounding factor that had the potential to inappropriately skew the results; therefore, the experiment was initiated with the intention of excluding data from any mouse that died during the experiment. We excluded 0 to 4 mice per treatment.

In the case of measurements in which variation among experiments tends to be low (for example, HSC frequency) we generally examined 3 to 6 mice. In the case of measurements in which variation among experiments tends to be higher (for example, reconstitution assays) we examined larger numbers of mice (>10). In the case of assays to assess protein synthesis, there were no historical data on which to base sample sizes, and we therefore performed multiple independent experiments with multiple biological replicates to ensure the reproducibility of our findings.

42. Groszer, M. *et al.* PTEN negatively regulates neural stem cell self-renewal by modulating G0-G1 cell cycle entry. *Proc. Natl Acad. Sci. USA* **103,** 111–116 (2006).
43. Kühn, R., Schwenk, F., Aguet, M. & Rajewsky, K. Inducible gene targeting in mice. *Science* **269,** 1427–1429 (1995).
44. Jonker, J. W. *et al.* The breast cancer resistance protein protects against a major chlorophyll-derived dietary phototoxin and protoporphyria. *Proc. Natl Acad. Sci. USA* **99,** 15649–15654 (2002).
45. Jacks, T. *et al.* Tumor spectrum analysis in p53-mutant mice. *Curr. Biol.* **4,** 1–7 (1994).
46. Akashi, K., Traver, D., Miyamoto, T. & Weissman, I. L. A clonogenic common myeloid progenitor that gives rise to all myeloid lineages. *Nature* **404,** 193–197 (2000).
47. Hardy, R. R., Carmack, C. E., Shinton, S. A., Kemp, J. D. & Hayakawa, K. Resolution and characterization of pro-B and pre-pro-B cell stages in normal mouse bone marrow. *J. Exp. Med.* **173,** 1213–1225 (1991).

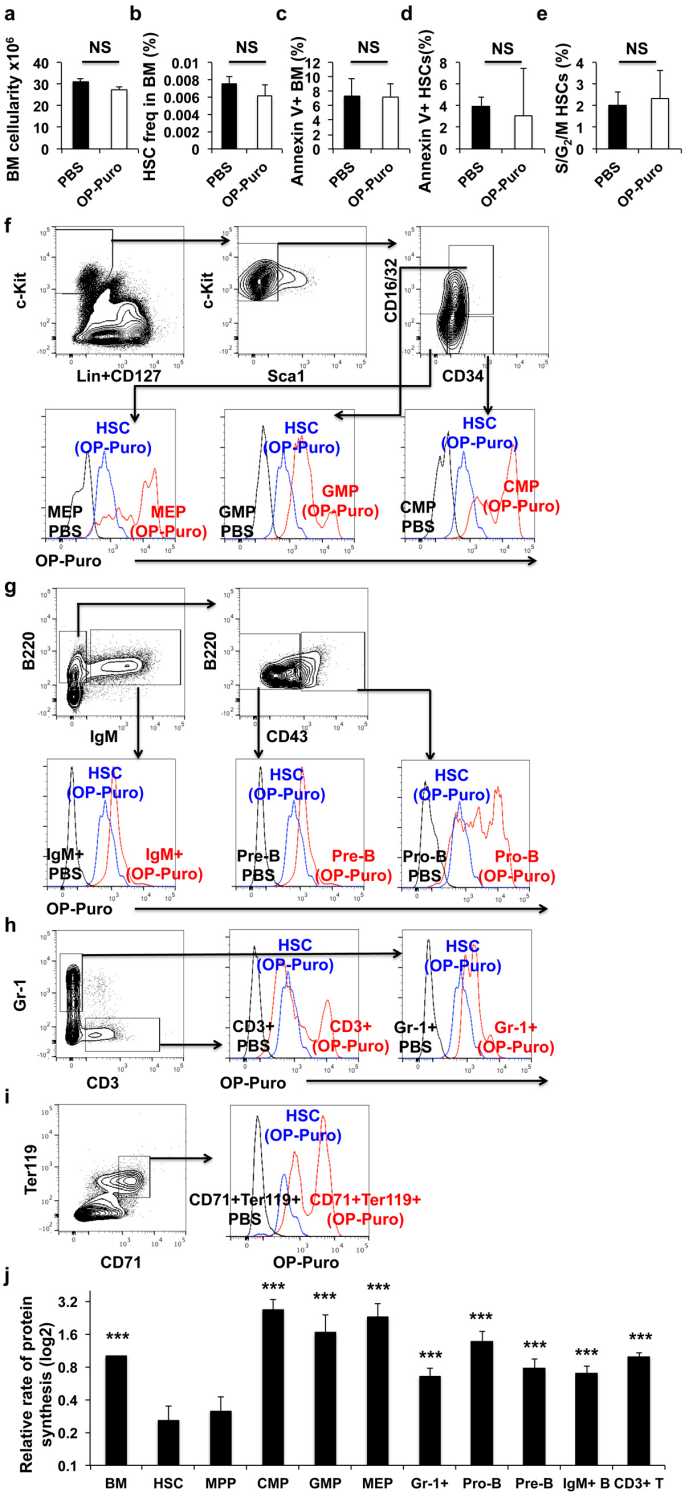

Extended Data Figure 1 | Isolation of haematopoietic progenitor cell populations by flow cytometry and histograms showing protein synthesis *in vivo* relative to HSCs from the same mice. **a**–**e**, One hour after OP-Puro administration to mice we observed no effect on bone marrow cellularity (one femur and one tibia (**a**); $n = 7$ PBS treated and $n = 9$ OP-Puro treated mice) or the frequencies of $CD150^{+}CD48^{-}$LSK HSCs (**b**; $n = 4$ PBS treated, $n = 6$ OP-Puro treated mice), annexin V^{+} bone marrow cells (**c**; $n = 4$ PBS treated mice, $n = 6$ OP-Puro treated mice), annexin V^{+} HSCs (**d**; $n = 4$ PBS treated mice, $n = 6$ OP-Puro treated mice), or HSCs in $S/G_2/M$ phase of the cell cycle (**e**; $n = 3$ mice per treatment; **a**–**e** each reflect two or three independent experiments). **f**–**i**, Representative flow-cytometry plots showing the markers and gating strategies used to isolate CMPs[46], GMPs[46], and MEPs[46] (**f**), pro-B[47], pre-B[47] and IgM^{+} B cells (**g**), Gr-1^{+} myeloid cells (**h**), $CD3^{+}$ T cells (**h**) and $CD71^{+}Ter119^{+}$ erythroid progenitors (**i**). Each panel also shows OP-Puro incorporation histograms for each cell population relative to HSCs after 1 h of OP-Puro incorporation *in vivo*. The level of background fluorescence from PBS treated controls is overlaid in black. **j**, Data from Fig. 1h showing protein synthesis in various haematopoietic-cell populations relative to unfractionated bone marrow cells on a $\log_2$ scale ($n = 15$ mice from 9 independent experiments). All data represent mean ± s.d. Two-tailed Student's *t*-tests were used to assess statistical significance in **a**–**e**. The statistical significance of differences relative to HSCs in **j** was assessed using a repeated-measures one-way ANOVA followed by Dunnett's test for multiple comparisons. Asterisks indicate statistical comparison to HSCs ($*P < 0.05$, $**P < 0.01$, $***P < 0.001$).

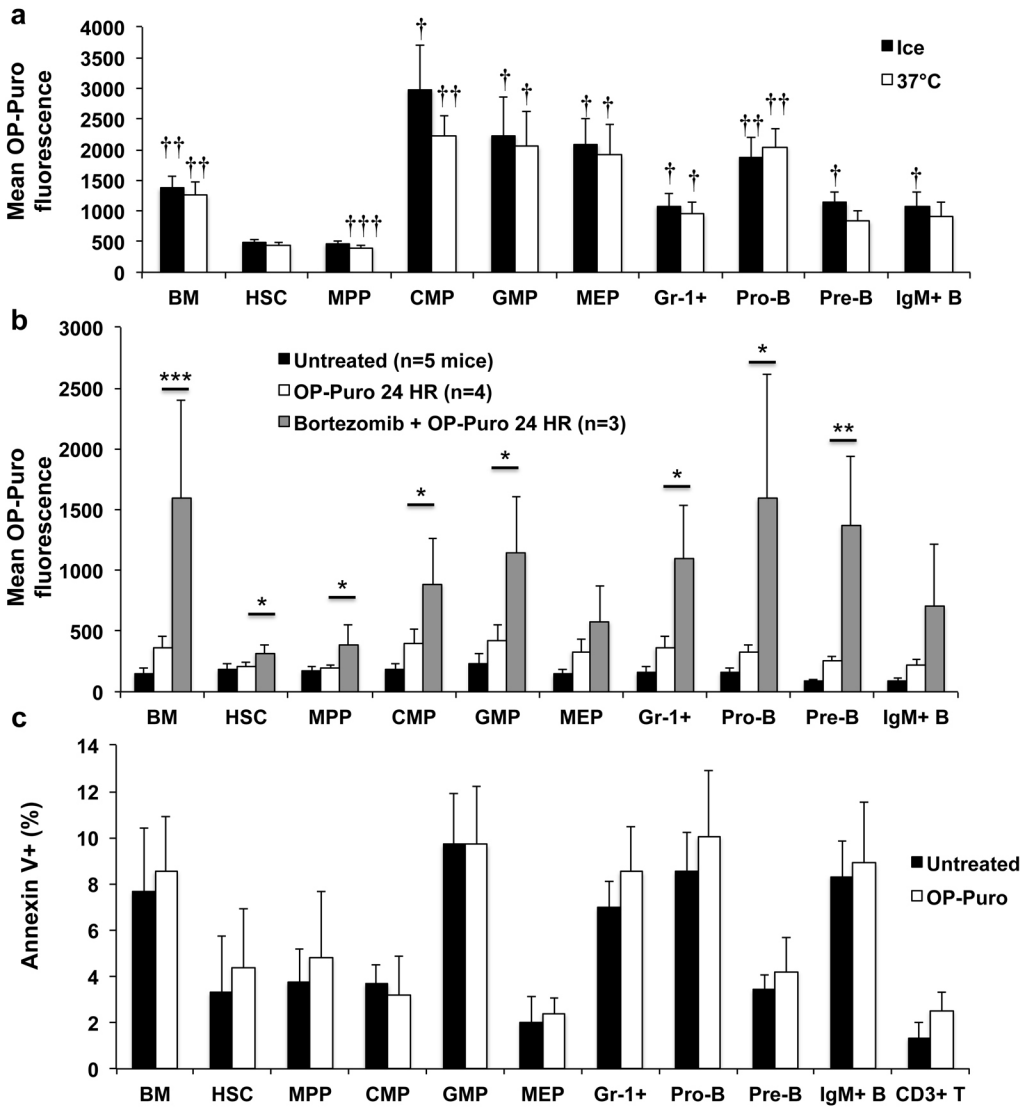

Extended Data Figure 2 | OP-Puro-containing polypeptides are not degraded within 30 min, the degradation that occurs over 24 h is blocked by bortezomib, and OP-Puro administration does not induce cell death. **a**, OP-Puro fluorescence in haematopoietic cells after 1 h of OP-Puro administration *in vivo* followed by a 30-min *ex vivo* incubation on ice or at 37 °C ($n = 11$ mice from 4 independent experiments). **b**, OP-Puro fluorescence in haematopoietic cells 24 h after OP-Puro administration *in vivo*. Treatment with bortezomib 1 h before OP-Puro administration increased OP-Puro fluorescence in every cell population 24 h later ($n = 3$ independent experiments; total number of mice per treatment are shown in the panel). **c**, Frequency of annexin V^+ cells in each cell population 1 h after OP-Puro administration *in vivo* relative to the same cells from untreated mice ($n = 7$ mice per treatment from 2 independent experiments). All data represent mean ± s.d. To assess the statistical significance of treatment effects within the same cell population we performed two-tailed Student's *t*-tests ($^*P < 0.05$, $^{**}P < 0.01$, $^{***}P < 0.001$). To assess the statistical significance of differences between HSCs and other cell populations in **a**, we performed a repeated-measures one-way ANOVA followed by Dunnett's test for multiple comparisons ($\dagger P < 0.05$, $\dagger\dagger P < 0.01$, $\dagger\dagger\dagger P < 0.001$).

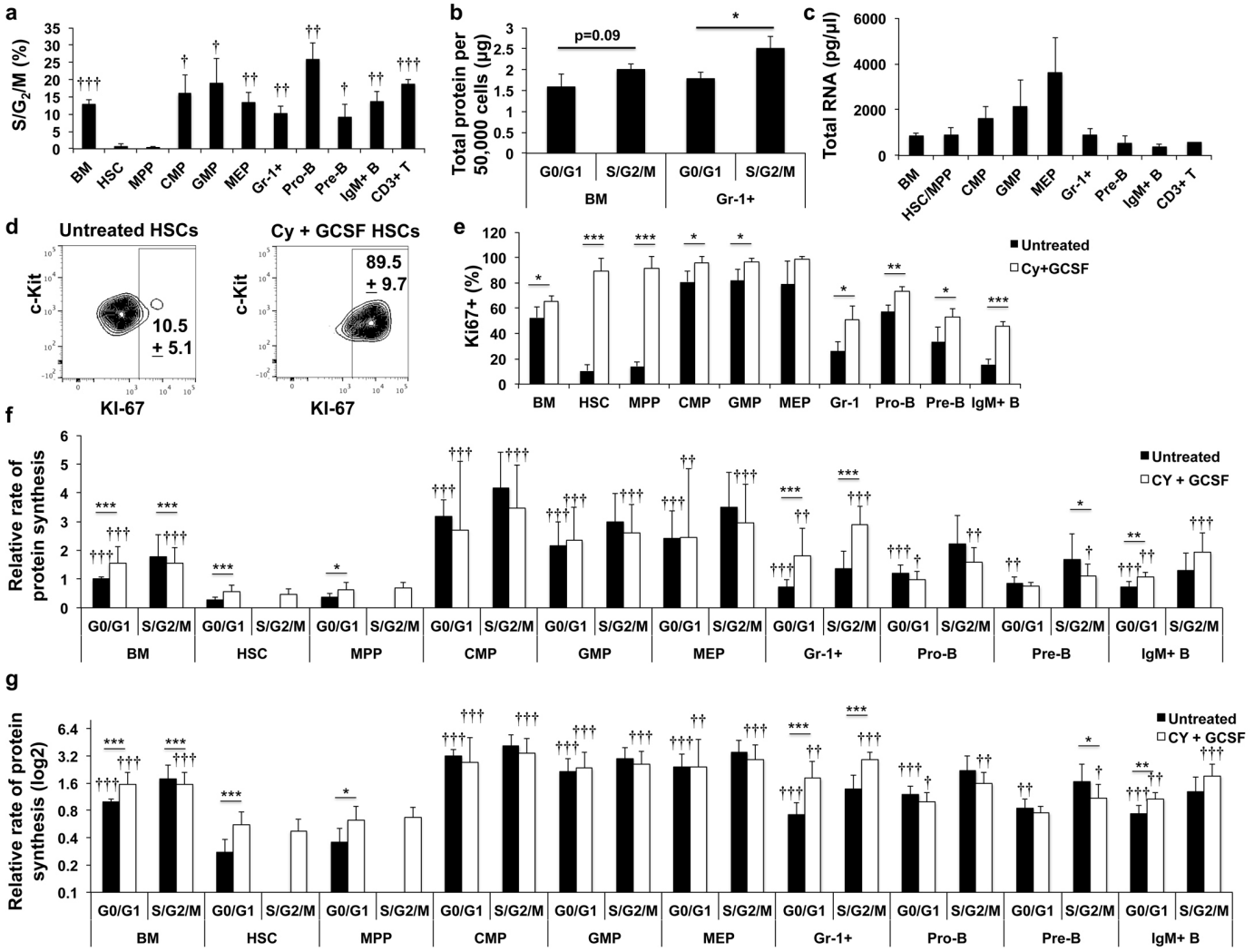

Extended Data Figure 3 | Cyclophosphamide and GCSF treatment drives certain cells into cycle and increases protein synthesis. **a**, Frequency of dividing cells in S/G_2/M phases of the cell cycle (>2N (>diploid) DNA content; $n = 5$ mice from 3 independent experiments). **b**, Total protein isolated from 50,000 unfractionated bone marrow cells or Gr-1$^+$ cells in G_0/G_1 or S/G_2/M measured by BCA assay ($n = 3$). **c**, Total RNA content in 15,000 cells from each stem- or progenitor-cell population ($n = 3$ mice). **d**, The frequency of cycling (KI-67$^+$) HSCs increased dramatically after treatment with cyclophosphamide (Cy) and GCSF ($n = 5$ untreated mice and $n = 6$ mice treated with cyclophosphamide and GCSF, from 2 independent experiments, $P < 0.001$). **e**, Frequency of KI-67$^+$ cells in haematopoietic-cell populations before and after treatment with cyclophosphamide and GCSF ($n = 5$ untreated mice and $n = 6$ mice treated with cyclophosphamide and GCSF for BM, HSC and MPP, $n = 3$ mice per treatment for other cell populations). **f**, **g**, Protein synthesis in G_0/G_1 and S/G_2/M cells from untreated mice or mice treated with cyclophosphamide followed by two days of GCSF ($n = 10$ mice per treatment from 6 independent experiments). These data are the same as shown in Fig. 3b, d, e, shown together in this panel for comparison. The data are plotted on a linear scale in **f** and on a $\log_2$ scale in **g**. All data represent mean ± s.d. To assess the statistical significance of treatment effects within the same cell population (**b**, **e**–**g**) we performed two-tailed Student's *t*-tests (*$P < 0.05$, **$P < 0.01$, ***$P < 0.001$). To assess the statistical significance of differences between HSCs and each other cell population (**a**, **c**, **f**, **g**) we performed a repeated-measures one-way ANOVA followed by Dunnett's test for multiple comparisons (†$P < 0.05$, ††$P < 0.01$, †††$P < 0.001$).

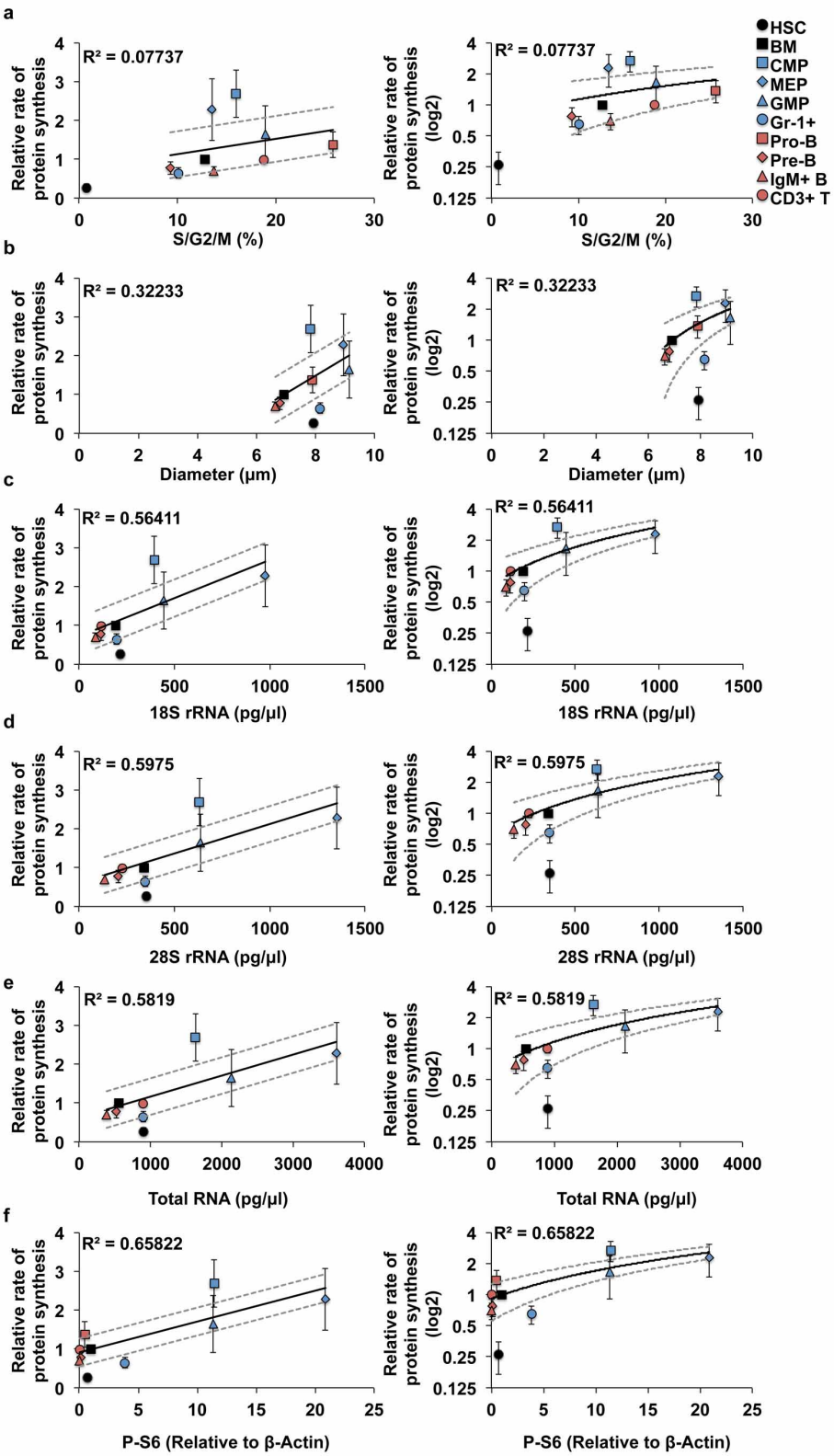

Extended Data Figure 4 | Differences in protein synthesis among haematopoietic stem and progenitor cells are not fully explained by differences in cell division, cell diameter, pS6 levels, rRNA or total RNA content. **a**–**f**, Scatter plots show the relative rates of protein synthesis (per hour) in each cell population (from Fig. 1h) plotted against the frequency of dividing cells (**a**; from Extended Data Fig. 3a), cell diameter (**b**; from Fig. 3f), 18S rRNA content (**c**; from Fig. 3g), 28S rRNA content (**d**; from Fig. 3g), total RNA content (**e**; from Extended Data Fig. 3c) and pS6 levels (**f**; from Fig. 5a normalized to β-actin). For each parameter, regressions were performed using all populations excluding HSCs and 95% confidence intervals were determined. R^2 values are shown in each plot. Rates of protein synthesis are plotted on a linear scale (left panels) and on a $\log_2$ scale (right panels). Note that HSCs were outliers with respect to each regression. $CD150^+CD48^-LSK$ cells were used to determine HSC rates of protein synthesis, cell diameter and percentage $S/G_2/M$, and $CD48^-LSK$ cells (HSCs and MPPs) were used to determine 18S, 28S, total RNA and pS6 levels (as these measurements required more cells). All data represent mean ± s.d.

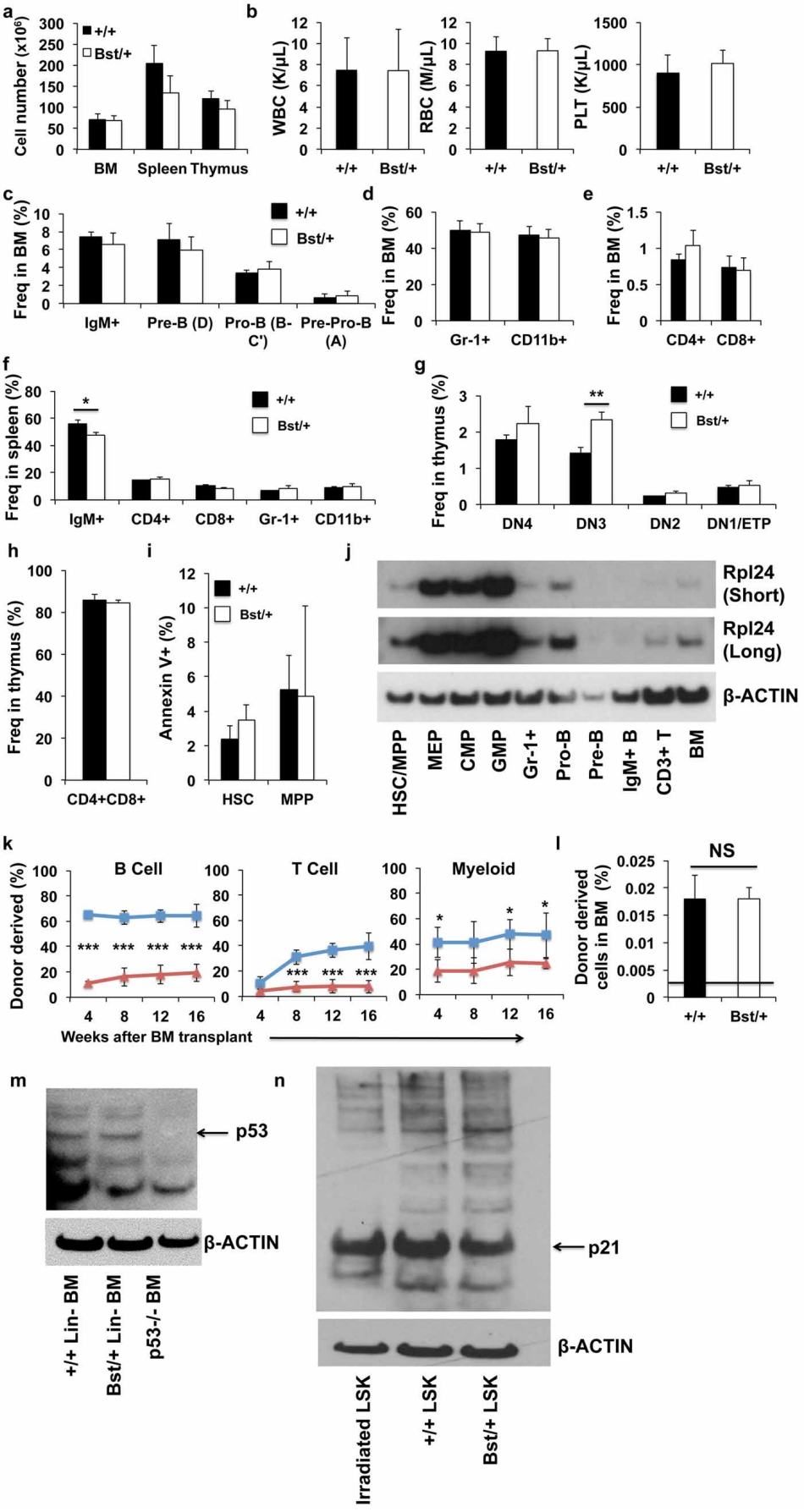

Extended Data Figure 5 | *Rpl24*$^{Bst/+}$ mice have normal frequencies of lymphoid and myeloid lineage progenitors and do not express increased p53 or p21^{Cip1} in adult haematopoietic cells. **a**, Bone marrow (2 femurs and 2 tibias; $n = 5$ wild-type and $n = 6$ *Rpl24*$^{Bst/+}$ mice from 4 experiments), spleen ($n = 3$ wild-type and $n = 4$ *Rpl24*$^{Bst/+}$ mice from 2 experiments), and thymus cellularity ($n = 3$ wild-type and $n = 4$ *Rpl24*$^{Bst/+}$ mice from 2 experiments). **b**, White blood cell, red blood cell and platelet counts ($n = 5$ wild-type and $n = 6$ *Rpl24*$^{Bst/+}$ mice from 4 experiments). **c**–**f**, The frequencies of B (**c**), myeloid (**d**) and T (**e**) lineage cells in the bone marrow and spleen (**f**) of *Rpl24*$^{Bst/+}$ and control mice ($n = 3$ wild-type and $n = 4$ *Rpl24*$^{Bst/+}$ mice from 2 experiments). **g**, **h**, The frequencies of T-lineage progenitors in the thymus of *Rpl24*$^{Bst/+}$ and control mice ($n = 3$ wild-type and $n = 4$ *Rpl24*$^{Bst/+}$ mice from 2 experiments). Double negative (DN)1 and early T-lineage progenitor (ETP) cells were $CD4^-CD8^-CD44^+CD25^-$; DN2 cells were $CD4^-CD8^-CD44^+CD25^+$; DN3 cells were $CD4^-CD8^-CD44^-CD25^+$; and DN4 cells were $CD4^-CD8^-CD44^-CD25^-$. **i**, The frequencies of annexin V^+ HSCs and MPPs in *Rpl24*$^{Bst/+}$ versus littermate control mice ($n = 3$ wild-type and $n = 4$ *Rpl24*$^{Bst/+}$ mice from 3 experiments). **j**, Western blot analysis for Rpl24 and β-actin using 30,000 cells from each haematopoietic-cell population. Differences in β-actin between lanes represent differences in β-actin content per cell (one representative blot from two independent experiments). **k**, Donor- B-cell, T-cell and myeloid-cell engraftment when 5×10^5 donor bone marrow cells were transplanted along with 5×10^5 recipient bone marrow cells into irradiated recipient mice ($n = 4$ independent experiments with a total of 17 recipients for wild-type cells and 20 for *Rpl24*$^{Bst/+}$ cells). These transplant recipients are the same as those shown in Fig. 4e. **l**, The frequency of donor cells in the bone marrow 20 h after transplanting 1×10^5 donor LSK cells from *Rpl24*$^{Bst/+}$ or wild-type control mice into irradiated recipient mice ($n = 3$ recipients per donor). The horizontal line represents the level of background detected in an untransplanted control. **m**, Western blot analysis for p53 using 5×10^5 $Lineage^-$ bone marrow cells from wild-type or *Rpl24*$^{Bst/+}$ mice, or 5×10^5 bone marrow cells from a *p53*$^{-/-}$ mouse (one representative blot from two experiments). **n**, Western blot analysis for p21^{Cip1} using 285,000 LSK cells from the bone marrow of adult wild-type or *Rpl24*$^{Bst/+}$ mice, or 142,500 LSK cells from a wild-type mouse that received 540 rad of total body irradiation 3 to 4 h before being euthanized (one representative blot from three independent experiments). All data represent mean ± s.d. Two-tailed Student's *t*-tests were used to assess statistical significance ($*P < 0.05$, $**P < 0.01$, $***P < 0.001$).

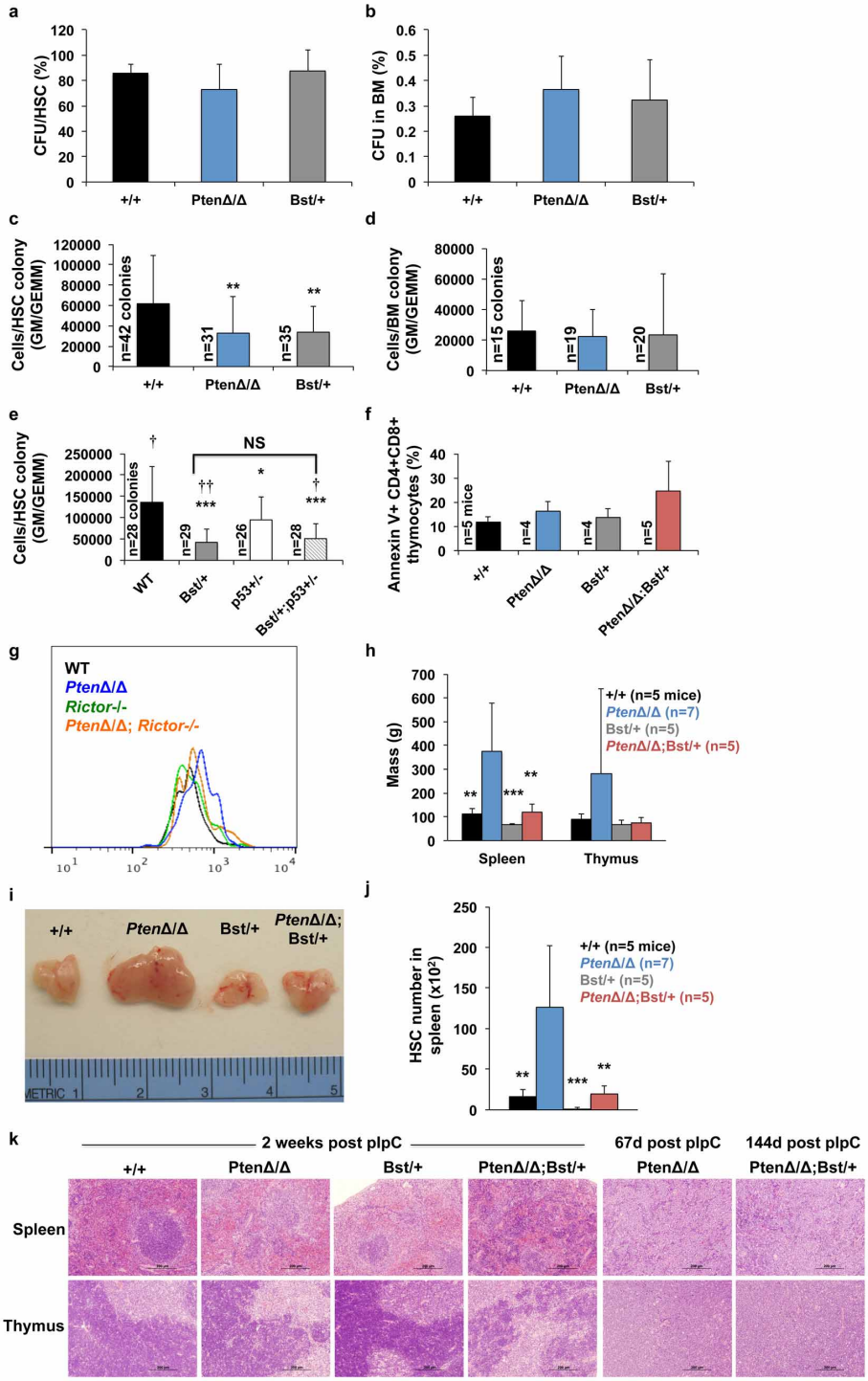

Extended Data Figure 6 | *Rpl24*$^{Bst/+}$ and *Pten*-deficient progenitors form colonies with normal cellularity but *Rpl24*$^{Bst/+}$ impairs the development of haematopoietic neoplasms after *Pten* deletion. **a**, **b**, The percentage of HSCs (**a**) or bone marrow cells (**b**) that formed colonies in methylcellulose within 14 days of culture ($n = 3$ mice per genotype in 3 independent experiments with 16 HSCs or 3,200 bone marrow cells tested per mouse per experiment). **c**, **d**, The average number of cells per granulocyte-monocyte (GM) or granulocyte, erythrocyte, monocyte, megakaryocyte (GEMM) colony derived from single HSCs (**c**) or bone marrow cells plated at clonal density (**d**) ($n = 4$ independent experiments). **e**, The average number of cells per GM or GEMM colony derived from individual HSCs of the indicated genotypes 15 days after plating ($n = 2$ independent experiments). **f**, Frequency of annexin V$^+$ CD4$^+$CD8$^+$ thymocytes ($n = 5$ independent experiments). **g**, Representative histograms of OP-Puro fluorescence in HSCs of the indicated genotypes. **h**, Mass of spleens and thymuses 2 weeks after pIpC administration ($n = 7$ independent experiments). **i**, Representative photographs of thymuses 2 weeks after pIpC administration to wild-type, *Mx1-Cre; Pten*$^{fl/fl}$, *Rpl24*$^{Bst/+}$ and *Mx1-Cre; Pten*$^{fl/fl}$; *Rpl24*$^{Bst/+}$ mice. **j**, HSCs in the spleen 2 weeks after pIpC administration ($n = 7$ independent experiments). **k**, Haematoxylin and eosin stained spleen and thymus sections from mice 2 weeks after pIpC administration or when they were killed owing to illness. All data represent mean ± s.d. In **a**–**d** and **f**, two-tailed Student's *t*-tests were used to assess statistical significance relative to wild-type; $*P < 0.05$, $**P < 0.01$. To assess statistical significance in **e** we performed a one-way ANOVA followed by Tukey's *t*-tests for multiple comparisons (relative to wild-type, $*P < 0.05$; $***P < 0.001$; and relative to $p53^{+/-}$, $\dagger P < 0.05$, $\dagger\dagger P < 0.01$). To compare the statistical significance of differences among genotypes in **h** and **j** we performed a one-way ANOVA followed by Dunnett's test for multiple comparisons relative to *Pten*-deficient ($**P < 0.01$, $***P < 0.001$).

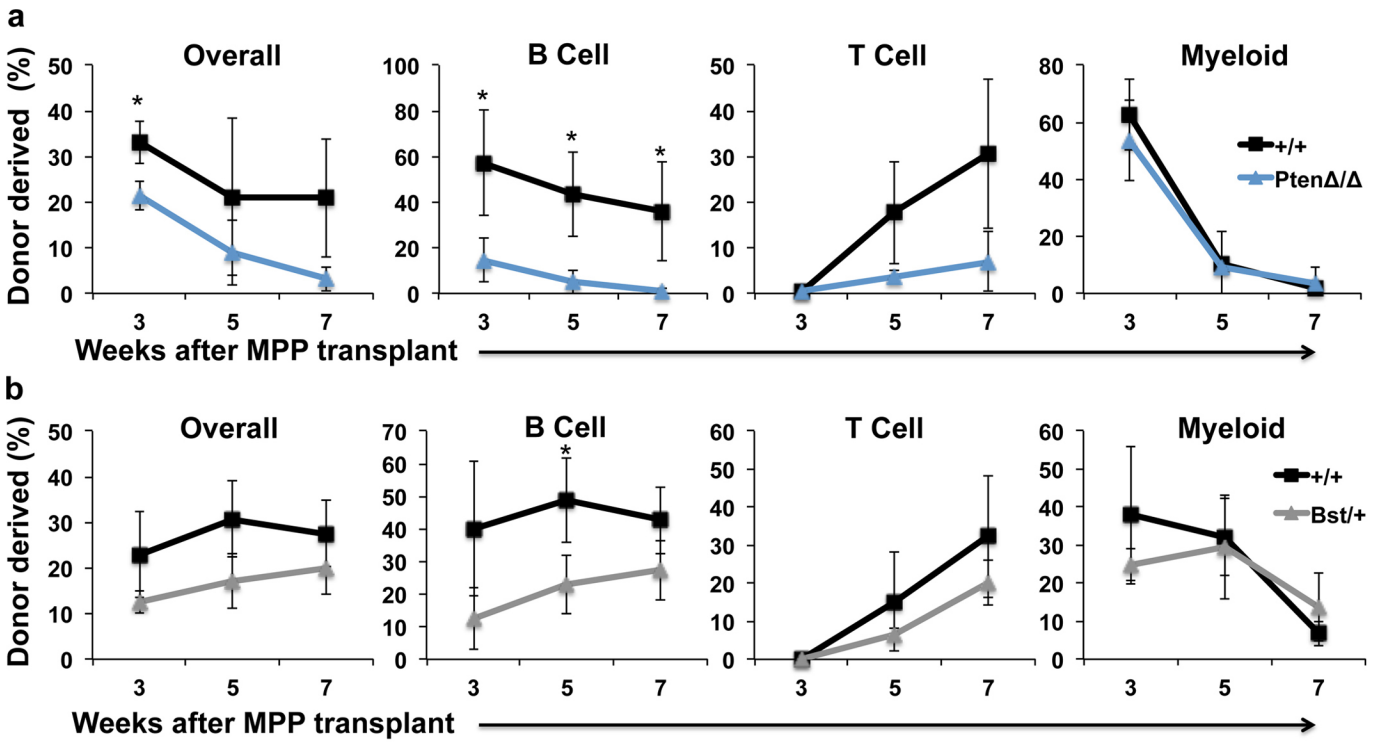

Extended Data Figure 7 | *Rpl24*$^{Bst/+}$ and *Pten*-deficient MPPs have relatively normal reconstituting activity. **a**, **b**, 100 donor CD150^{-}CD48^{-}LSK MPPs from *Mx1-Cre; Pten*$^{fl/fl}$ versus control mice (**a**; $n = 3$ independent experiments with a total of 13 recipients per genotype) or *Rpl24*$^{Bst/+}$ versus control mice (**b**; $n = 3$ independent experiments with a total of 14 recipients of wild-type cells and 13 recipients of *Rpl24*$^{Bst/+}$ cells) were transplanted along with 3×10^5 recipient-type bone marrow cells into irradiated recipient mice. Donor-cell engraftment levels in the peripheral blood were assessed at 3, 5 and 7 weeks after transplantation. All data represent mean ± s.d. Two-tailed Student's *t*-tests were used to assess statistical significance relative to wild-type; $^*P < 0.05$.